Study and optimization of a hybrid MPGD-based detector of single photons

Leonardo Benjamin Rizzuto

Supervisor:	Fulvio Tessarotto
Co-Supervisor:	Stefano Levorato
Internal Supervisor:	Anna Martin

Istituto Nazionale di Fisica Nucleare Trieste

Outline

- Brief introduction to COMPASS
- The novel Photon Detectors for COMPASS RICH-1
- Goals of the thesis
- Gain measurements
- Ion BackFlow measurements
- Conclusions

COMPASS: COmmon Muon and Proton Apparatus for Structure and Spectroscopy

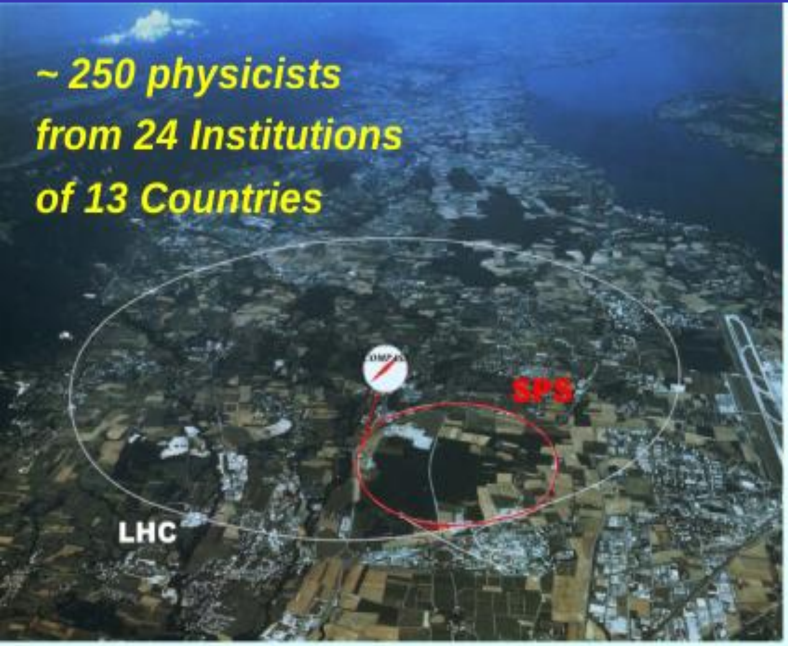

Дубна (LPP and LNP), Москва (INR, LPI, State University), Протвино

Warsawa (NCBJ), Warsawa (TU) Warsawa (U)

Praha (CU/CTU) Liberec (TU) Brno (ISI-ASCR)

Calcutta (Matriviani)

Taipei (AS)

CERN

Yamagata

Lisboa/Aveiro

Tel Aviv

Bochum, Bonn (ISKP & PI), Erlangen, Freiburg, Mainz, München TU

USA (UIUC)

Saclay

Torino (University, INFN), Trieste (University, INFN)

Experiments with muon beam:	*Experiments with hadron beams:*
COMPASS - I (2002 – 2011)	
Spin structure, Gluon polarization	*Pion polarizability*
Flavor decomposition	*Diffractive and Central production*
Transversity	*Light meson spectroscopy*
Transverse Momentum-dependent PDF	*Baryon spectroscopy*
COMPASS - II (2012 – 2020) …	
DVCS and HEMP	*Pion and Kaon polarizabilities*
Unpolarized SIDIS and TMDs	*Drell-Yan studies*

COMPASS: COmmon Muon and Proton Apparatus for Structure and Spectroscopy

The COMPASS spectrometer:

A 60 metre long fixed target experiment

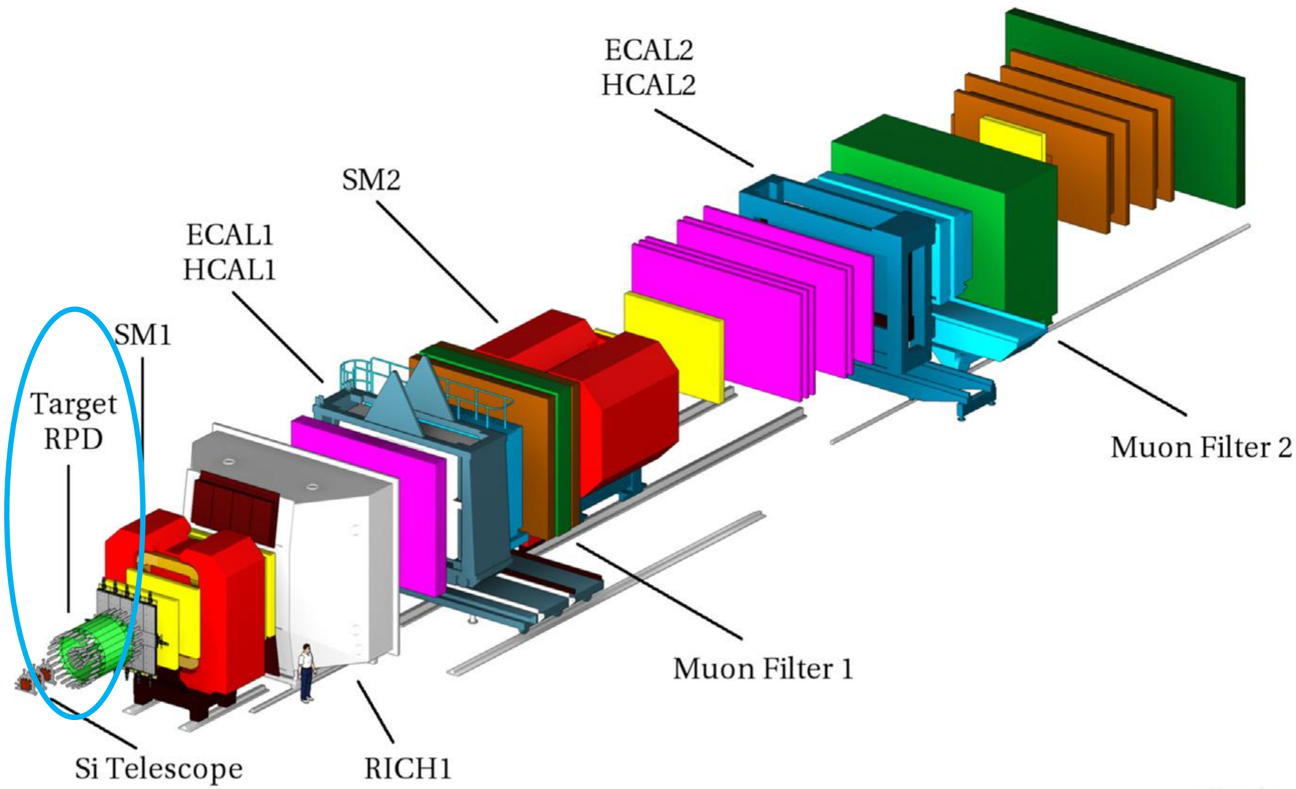

COMPASS: COmmon Muon and Proton Apparatus for Structure and Spectroscopy

The COMPASS spectrometer:

A 60 metre long fixed target experiment with two stages

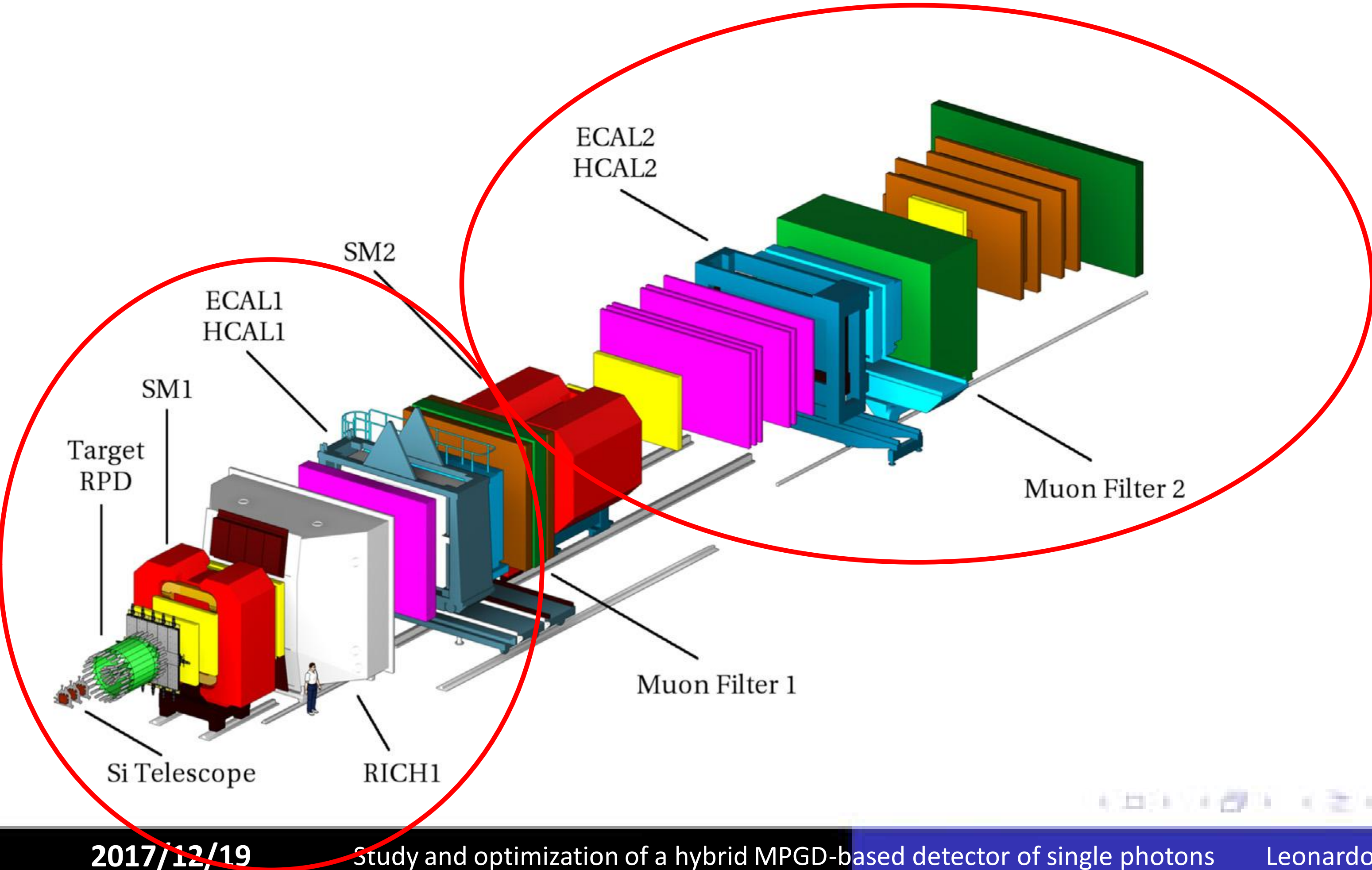

COMPASS: COmmon Muon and Proton Apparatus for Structure and Spectroscopy

The COMPASS RICH-1:

Hadron Identification in a momentum range 3-55 GeV/c

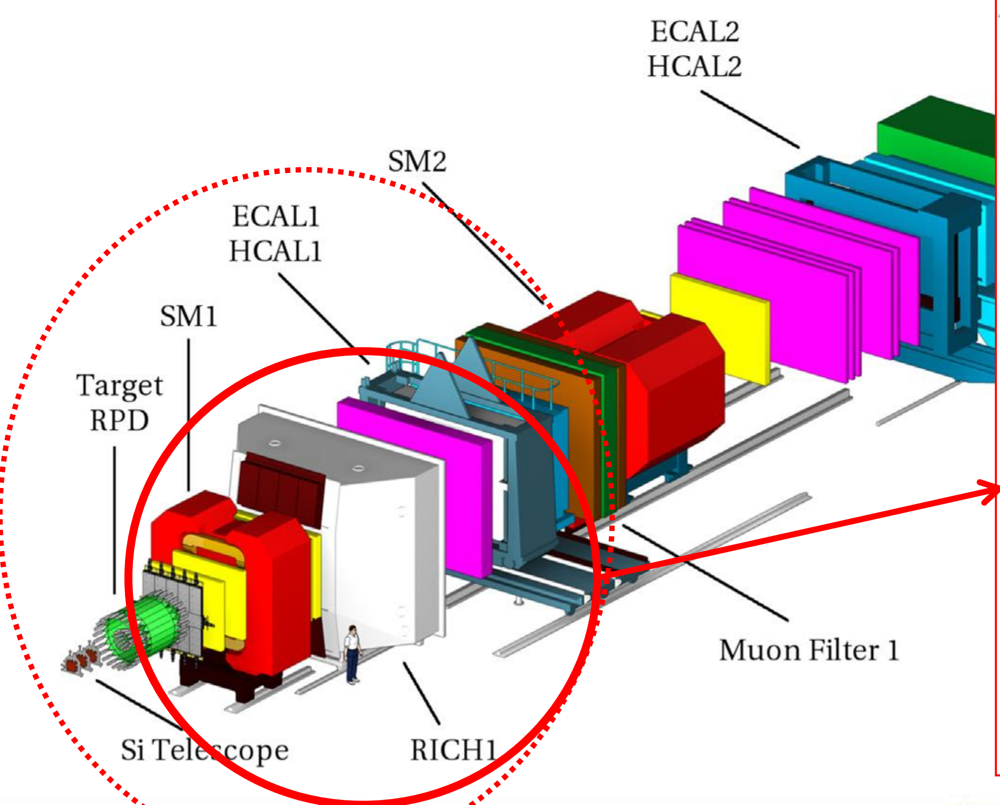

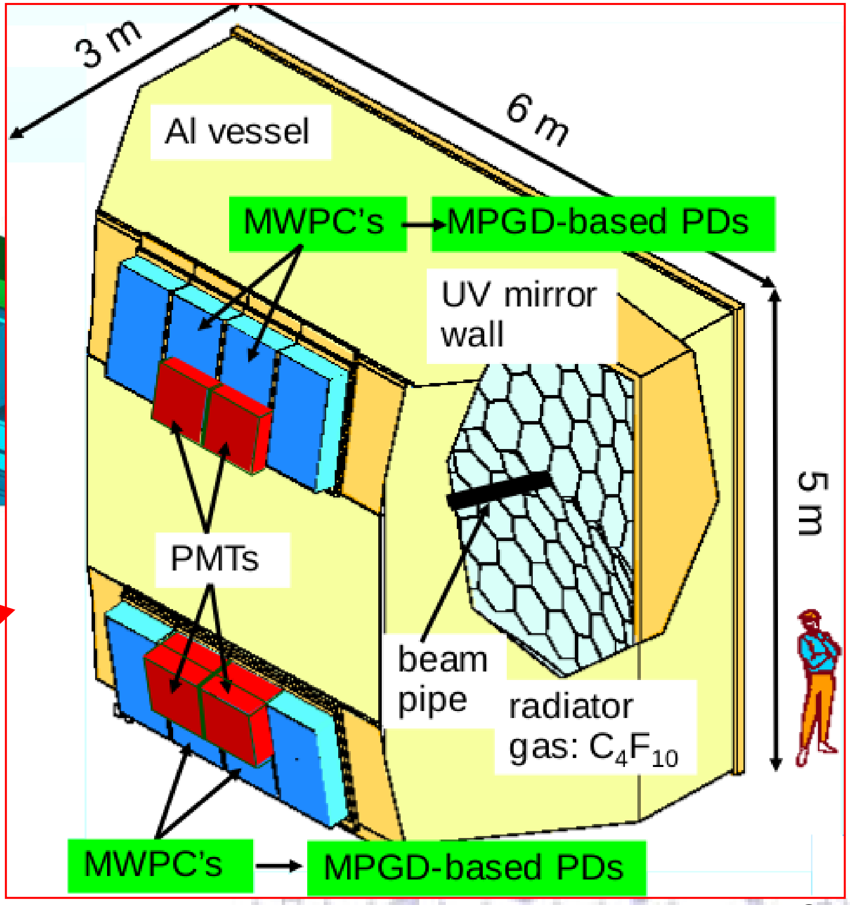

COMPASS: COmmon Muon and Proton Apparatus for Structure and Spectroscopy

The COMPASS RICH-1:

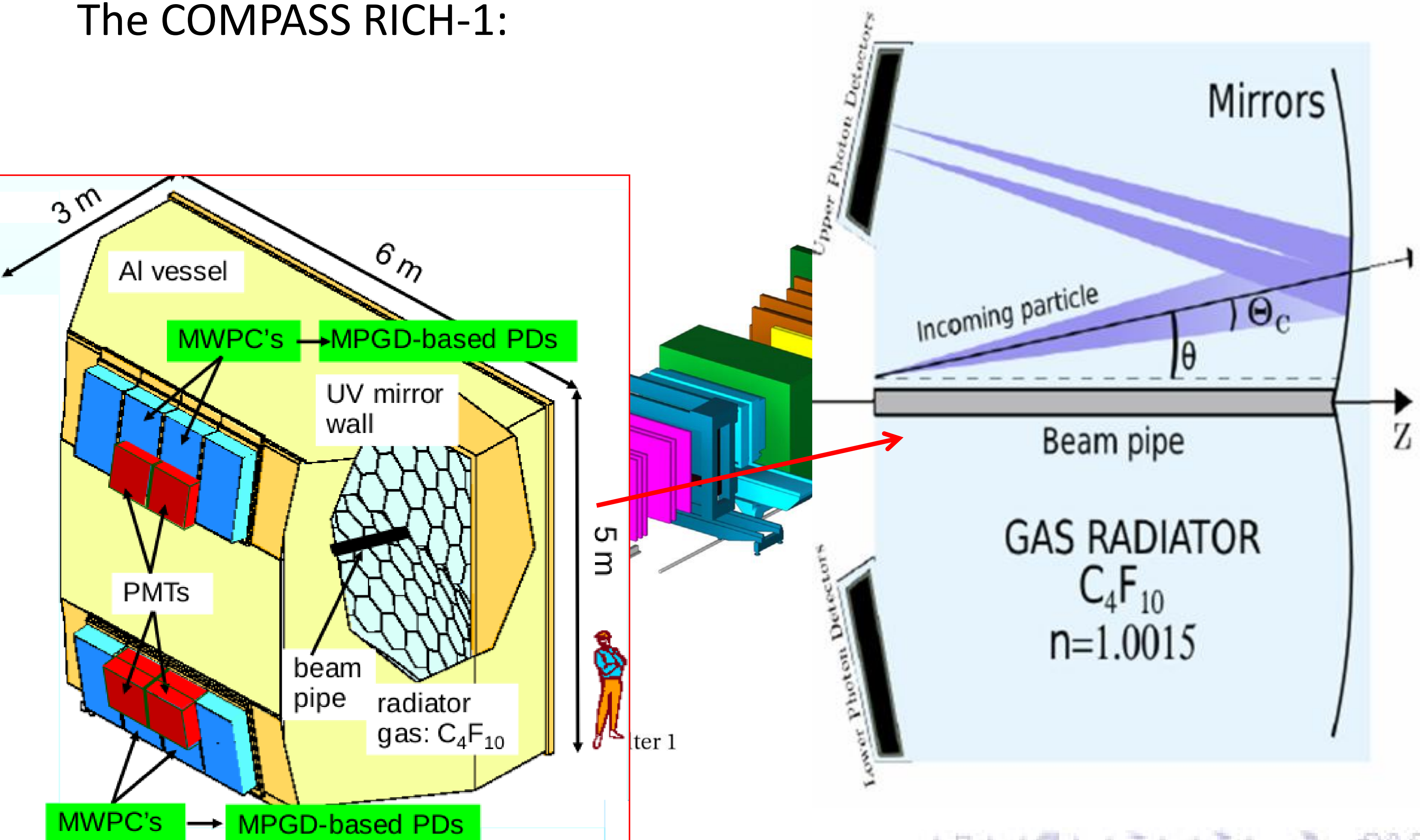

MWPC+CsI Photon Detectors

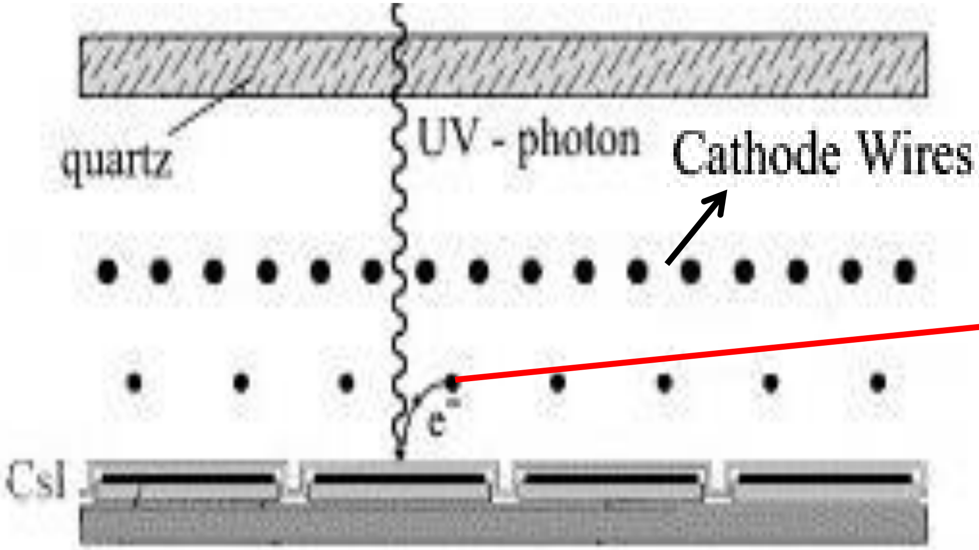

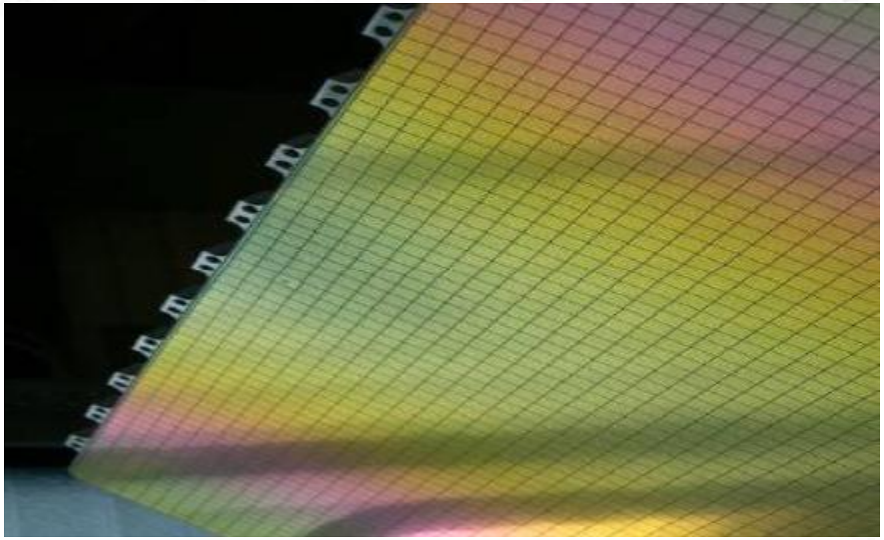

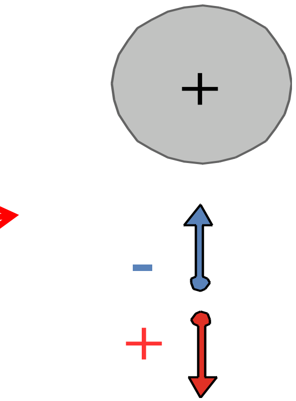

MWPC+CsI Photon Detectors

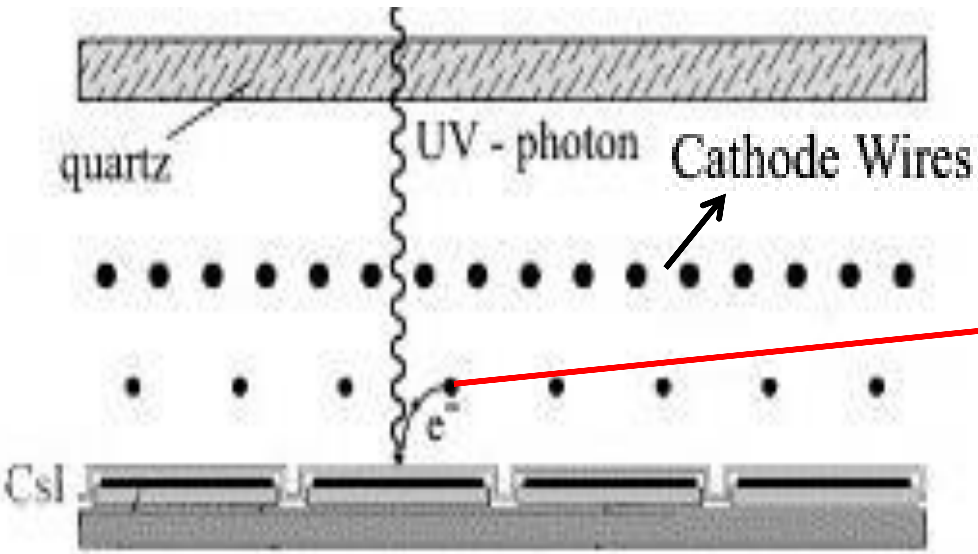

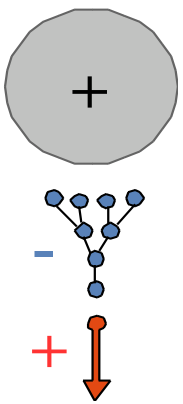

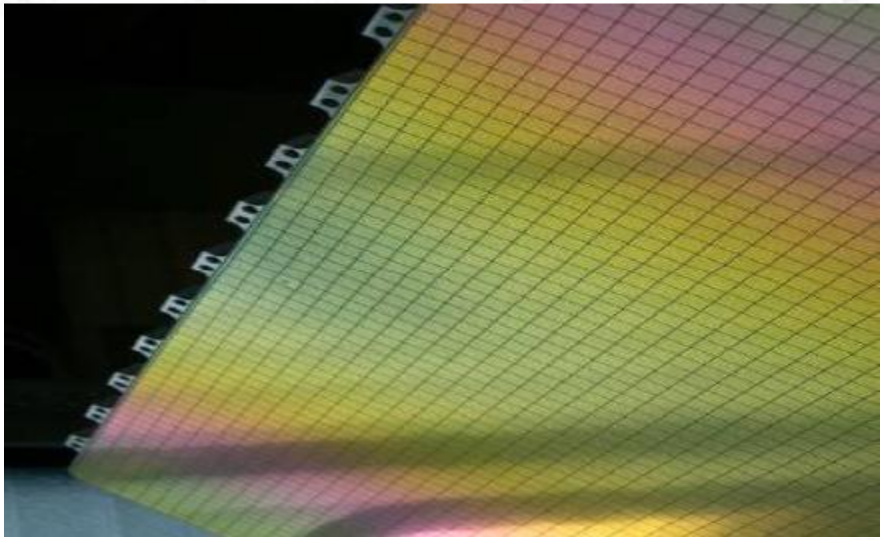

MWPC+CsI Photon Detectors

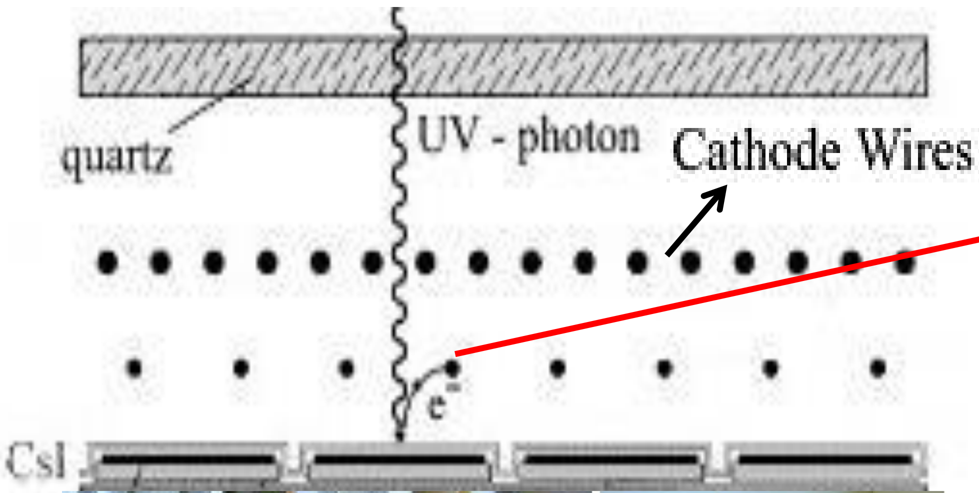

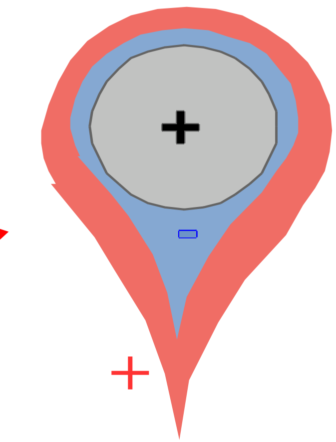

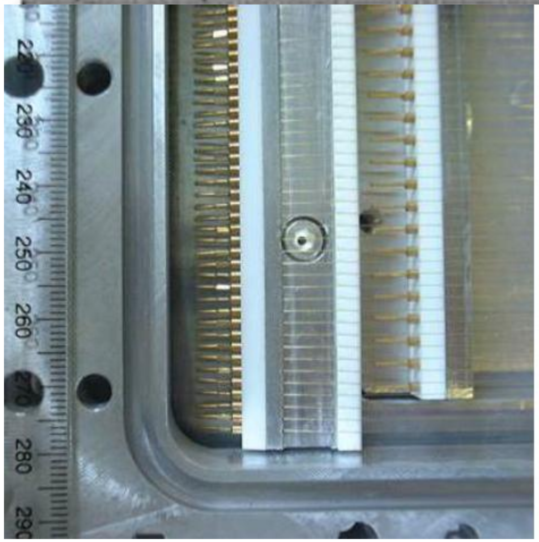

Ion BackFlow (IBF) > 50%

photocathode aging

(~mC/cm^2→*QE* degradation)

COMPASS RICH-1 PD UPGRADE

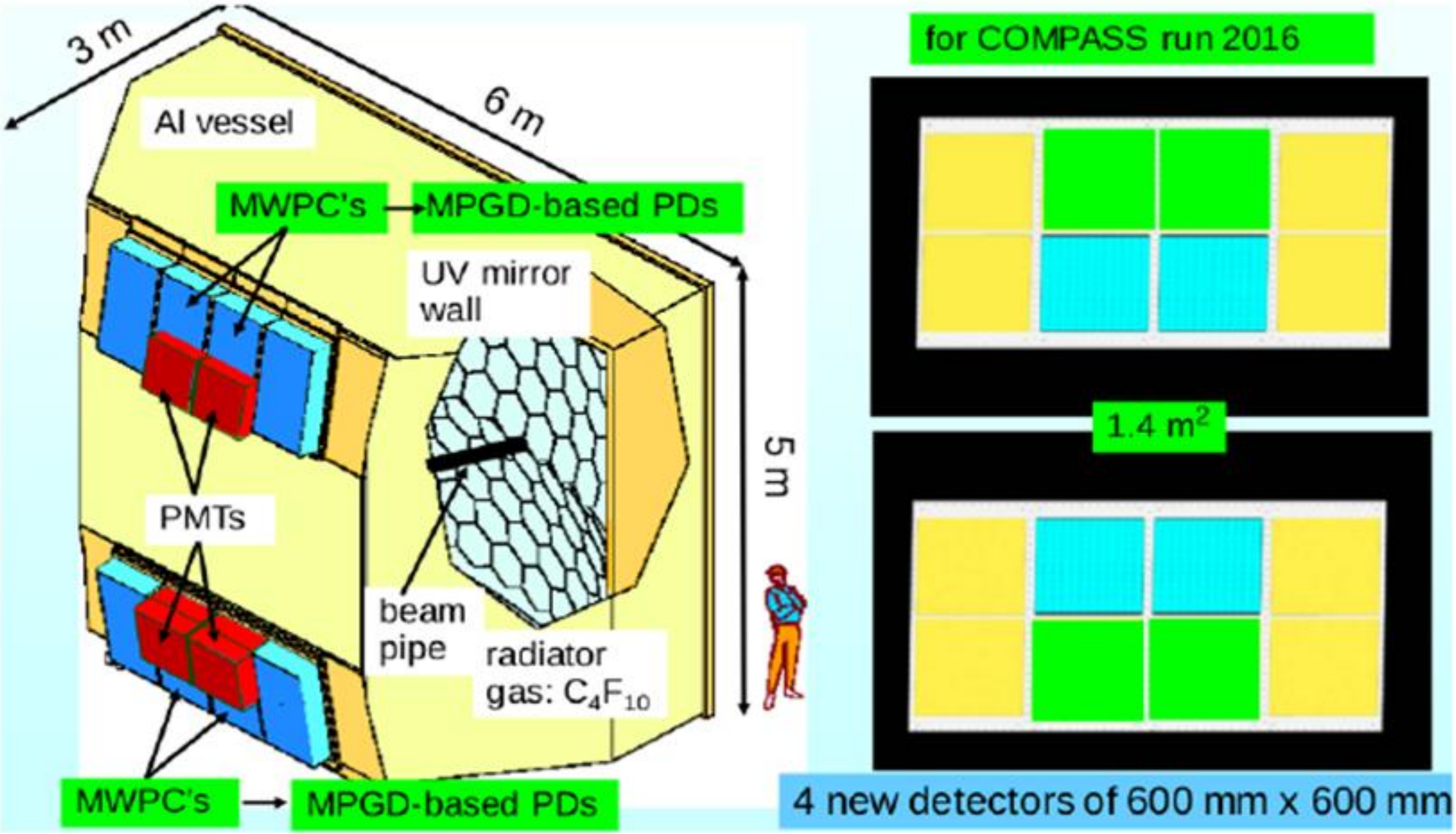

The new hybrid MPGD concept for RICH-1

For the first time of a hybrid MPGD architecture used in PDs of single photons in a running experiment .

(Result of 7 years of dedicated R&D)

Strong IBF suppression thanks:

- Staggered configuration
- Micromegas

The goal is IBF < 5%

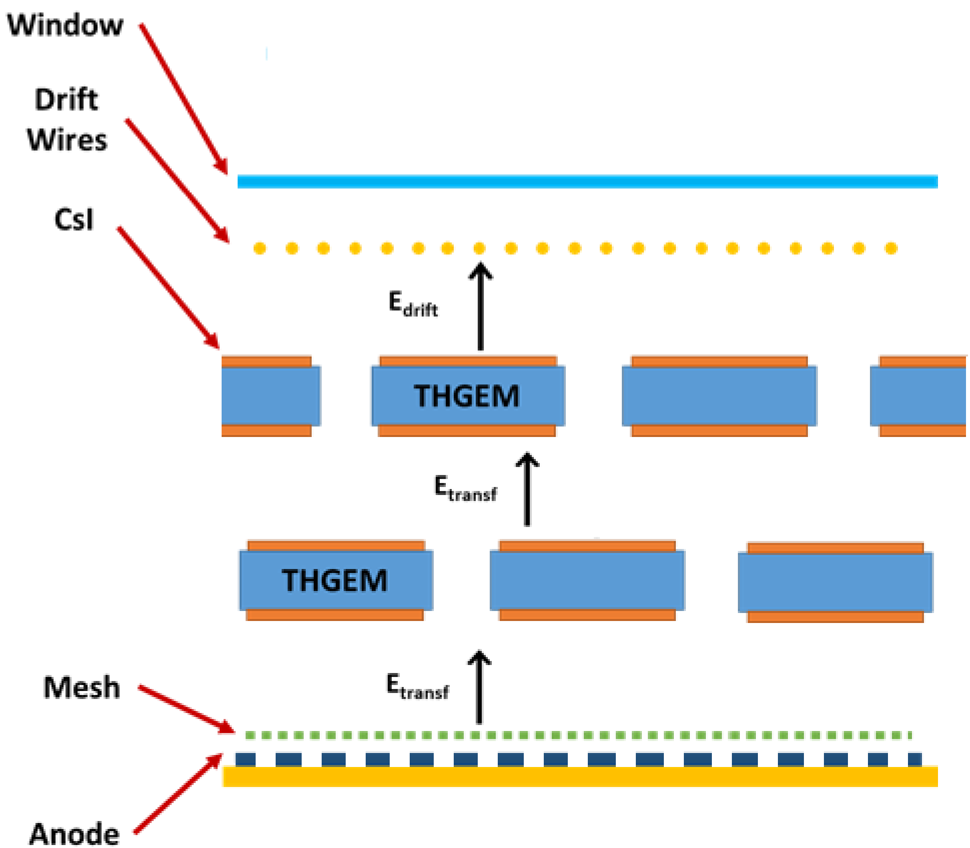

Operational settings:

ΔV_{THGEM1} = 1275 V ΔV_{THGEM1} = 1225 V

$E_{Transfer1}$ = 1 kV/cm $E_{Transfer2}$ = 0.6 kV/cm

$\Delta V_{Micromegas}$ = 624 V ΔV_{Drift} = 500 V

GEM: Gas Electron Multiplier

by F. Sauli (1997 CERN)

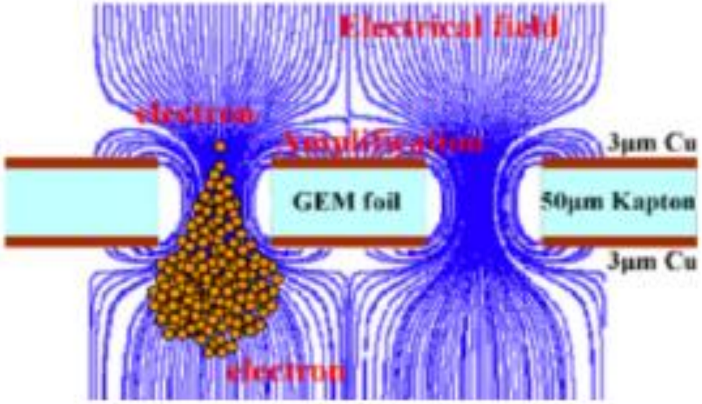

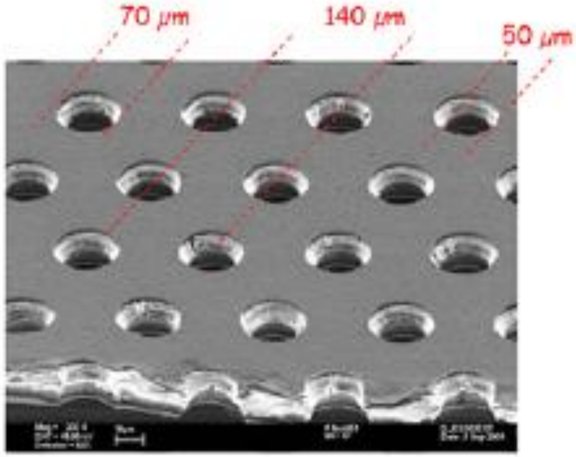

Innovative feature: easily shaped to match the experimental requirements.
"Standard GEM": 70 μm wide holes with 140 μm pitching, etched in a triangular pattern on 50 μm copper-clad kapton.

MPGD: Micro-Pattern Gaseous Detectors
THGEM-based Photon Detectors

Novel detector technologies based on PCB photolitography techniques (started in the '90s)

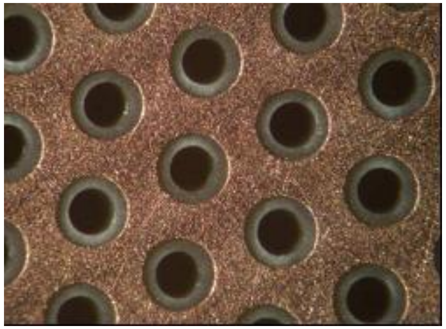

Thick GEM s (THGEMs):

regular pattern of holes with:

- thickness: t = 0.2 - 1 mm
- hole diameter: d = 0.2 - 1 mm
- hole pitch: p = 0.4 - 2 mm
- rim width: r = 0 - 0.1 mm

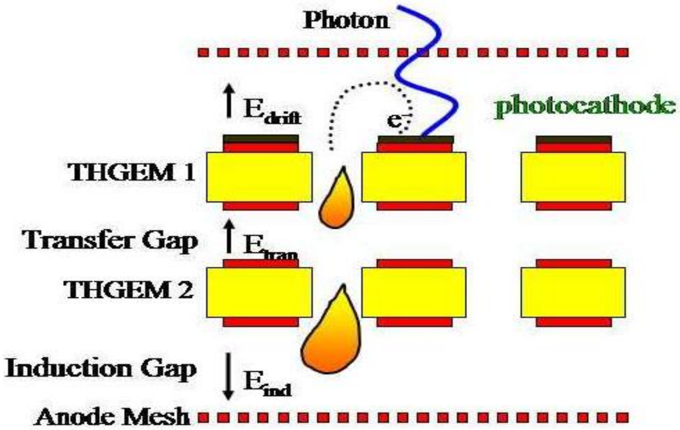

Micromegas: Micro-mesh Gaseous Structure

Thin parallel-plate avalanche counter: mesh very close (50 ÷ 150 μm) to the anode defines the multiplication gap.

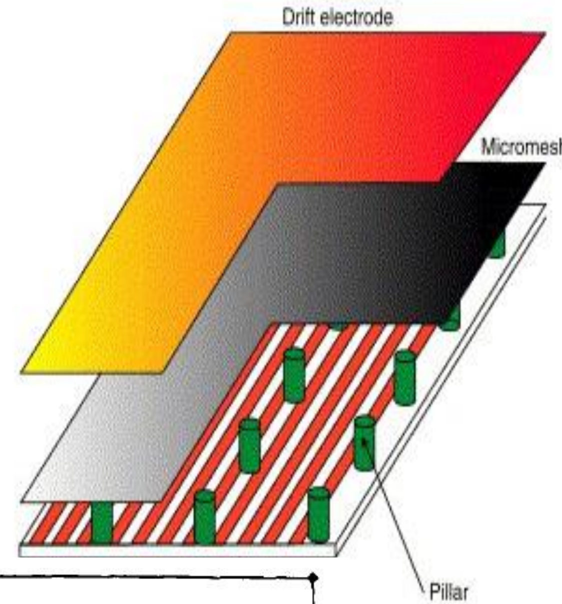

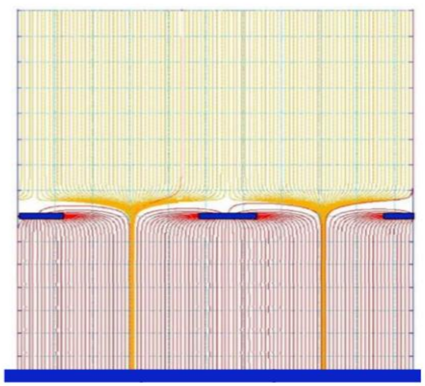

~ kV/cm

few mm

> 10 kV/cm

~ 100μm

Ion-blocking capability:

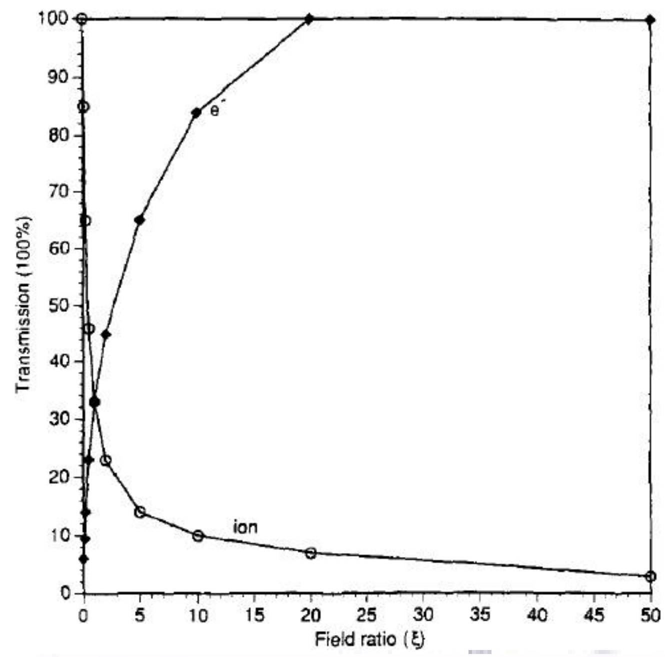

Goals of the Thesis

Some aspects of the performances achievable with the new hybrid MPGD archithecture cannot be studied operating the Photon Detectors on COMPASS RICH-1:

- **Individual contributions to the total Gain**
- **The Temperature-Pressure dependence of the Gain**
- **Accurate measurement of IBF to the photocathode**

The hybrid MPGD Prototype

The goal is to measure these quantities with a PD prototype featuring the same geometry of the new RICH-1 PDs.

Kapton window for ^{55}Fe

Quartz window for UV source

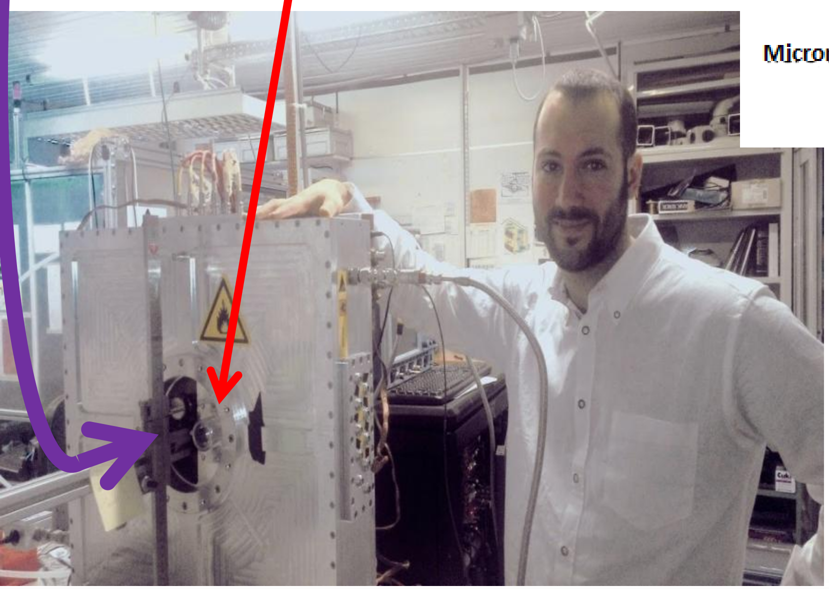

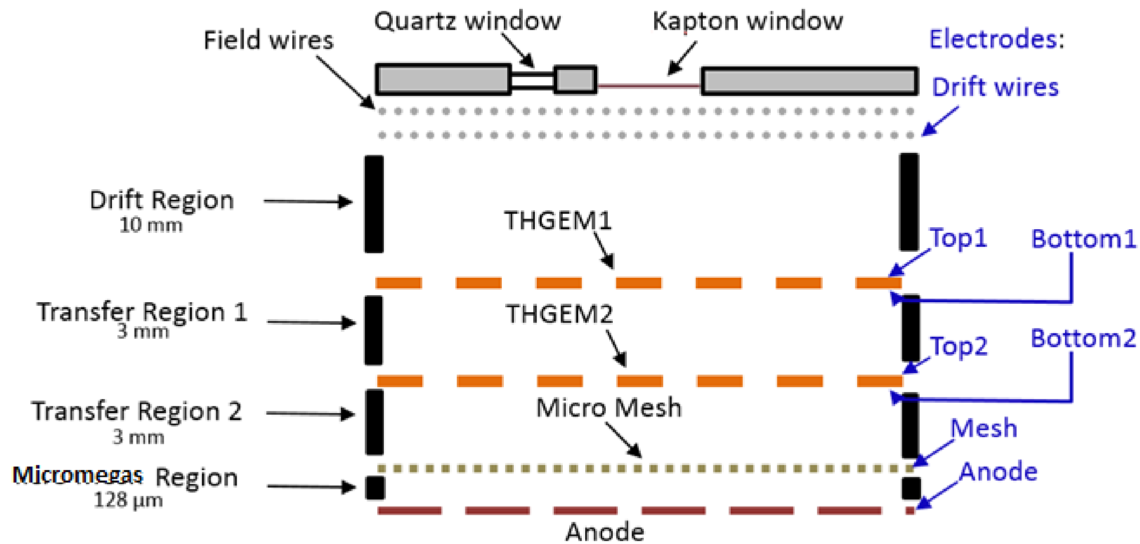

Experimental Setup used

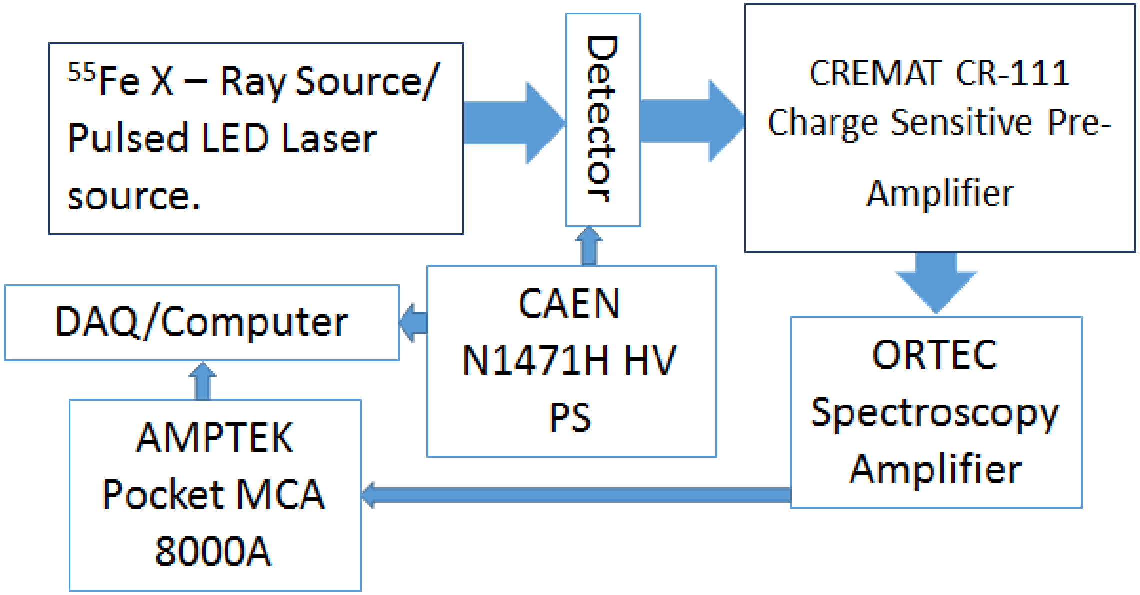

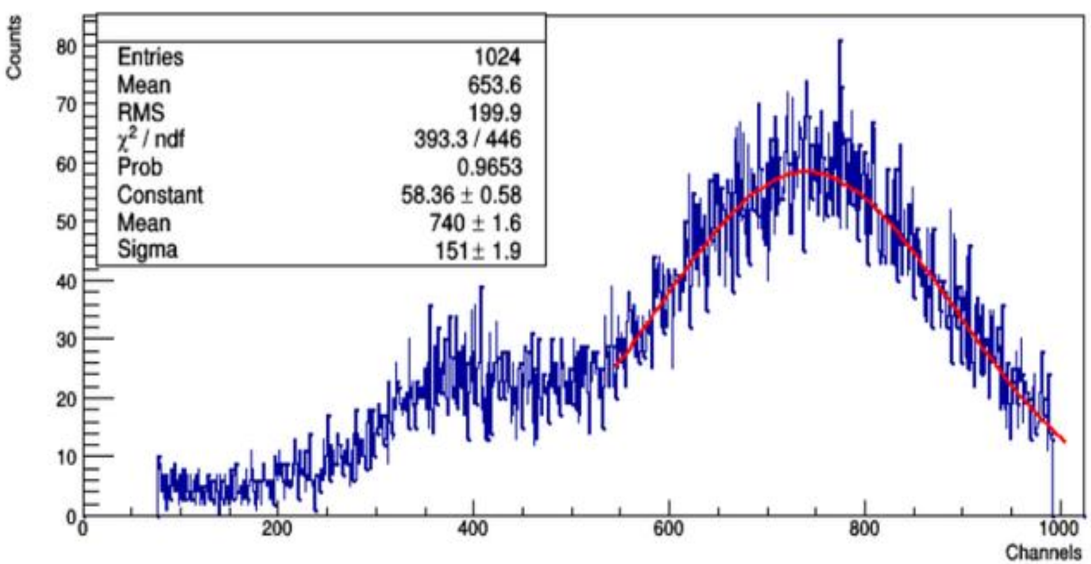

- Gain was measured fitting the main peak of ^{55}Fe source

Gain = n_e^{Peak} / $n_e^{prim.}$

Average number of electron-ion pairs generated:
In $Ar:CO_2$ 70:30 mixture: 207
In $Ar:CH_4$ 50:50 mixture: 226

Collection Efficiency study

I carefully studied the collection efficiency of primary electrons produced in the Drift region

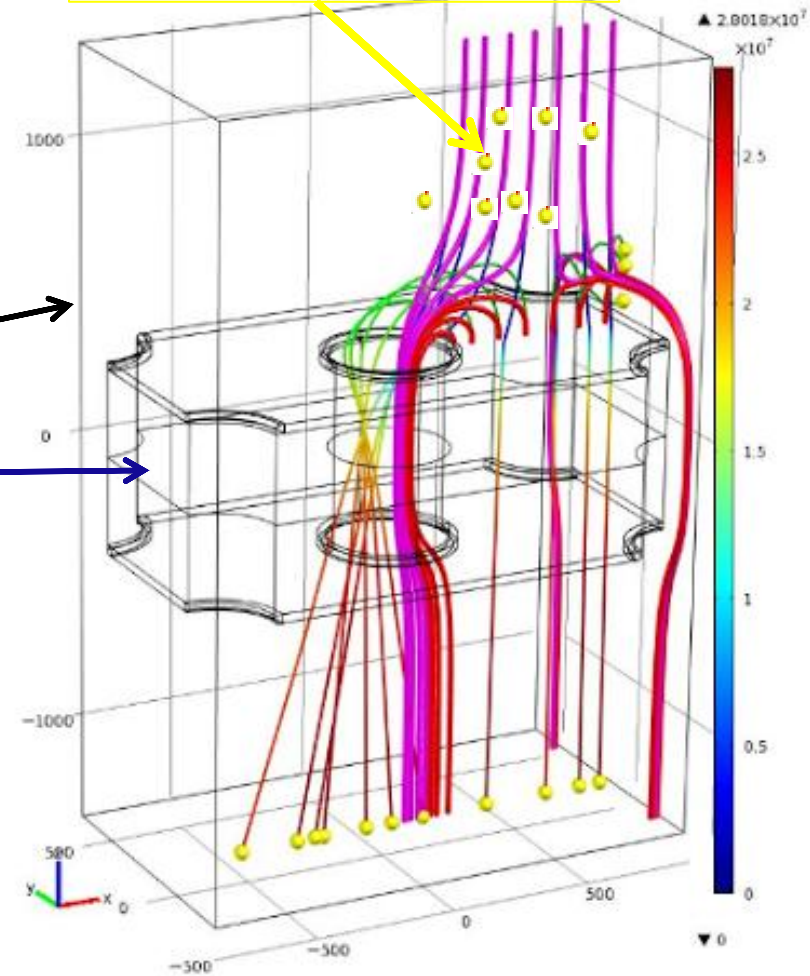

Collection Efficiency study

At fixed ΔV_{THGEM1}, applying $\Delta V_{drift} = 0.5 \div 2.5$ kV,

12 curves were obtained:

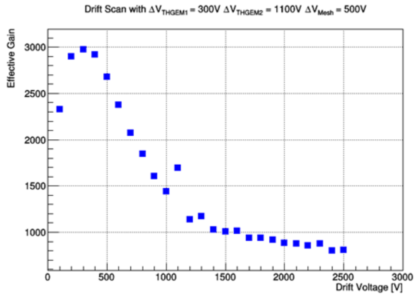

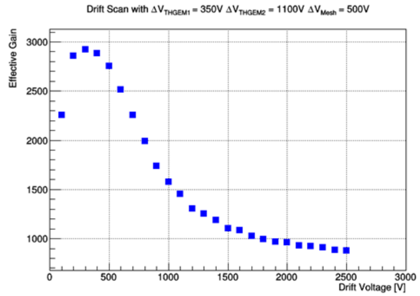

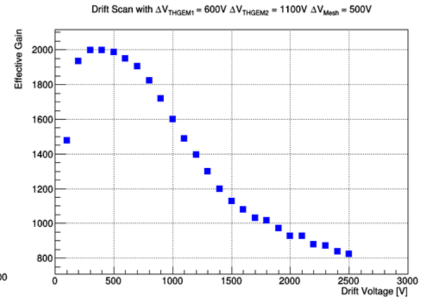

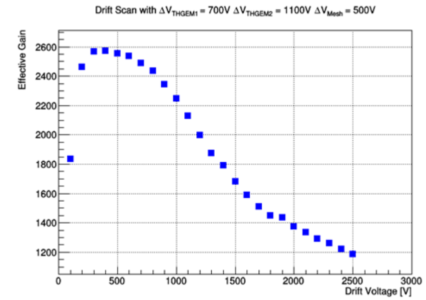

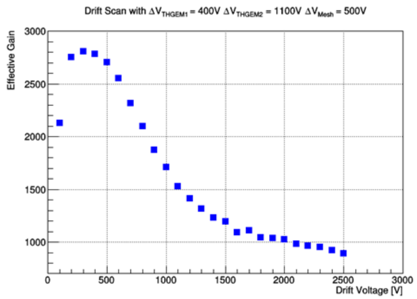

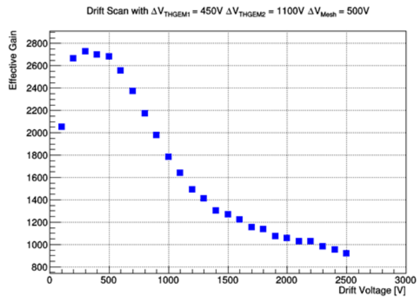

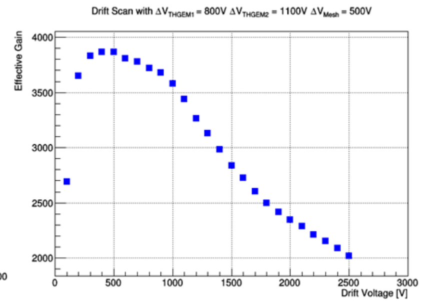

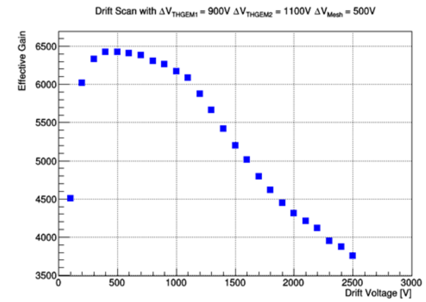

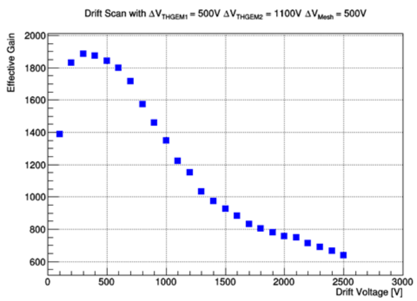

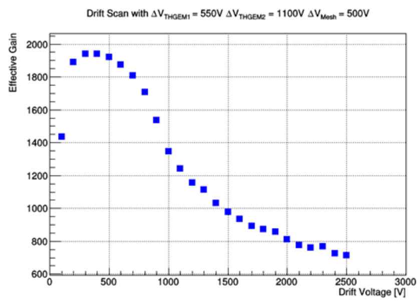

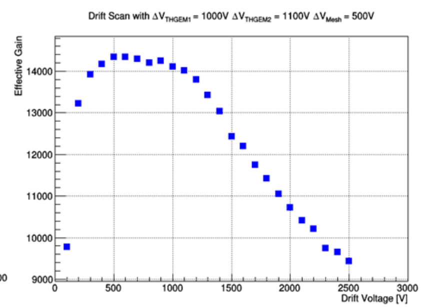

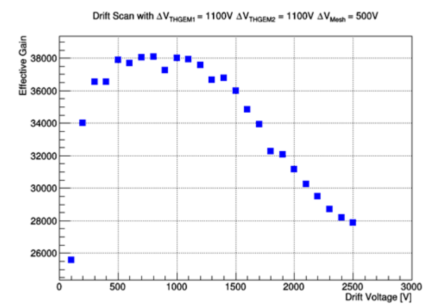

Collection Efficiency study

Collection Efficiency

is only due electrostatics

→ scaling

with $\Delta V_{Drift} / \Delta V_{THGEM1}$

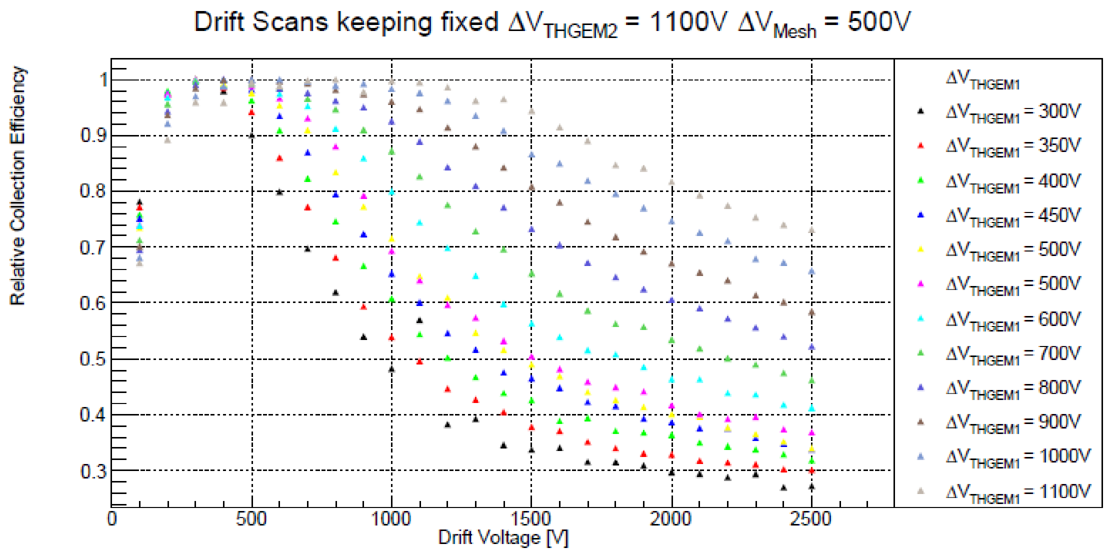

Max. Efficiency for

$\Delta V_{Drift} / \Delta V_{THGEM1} = 3/5$

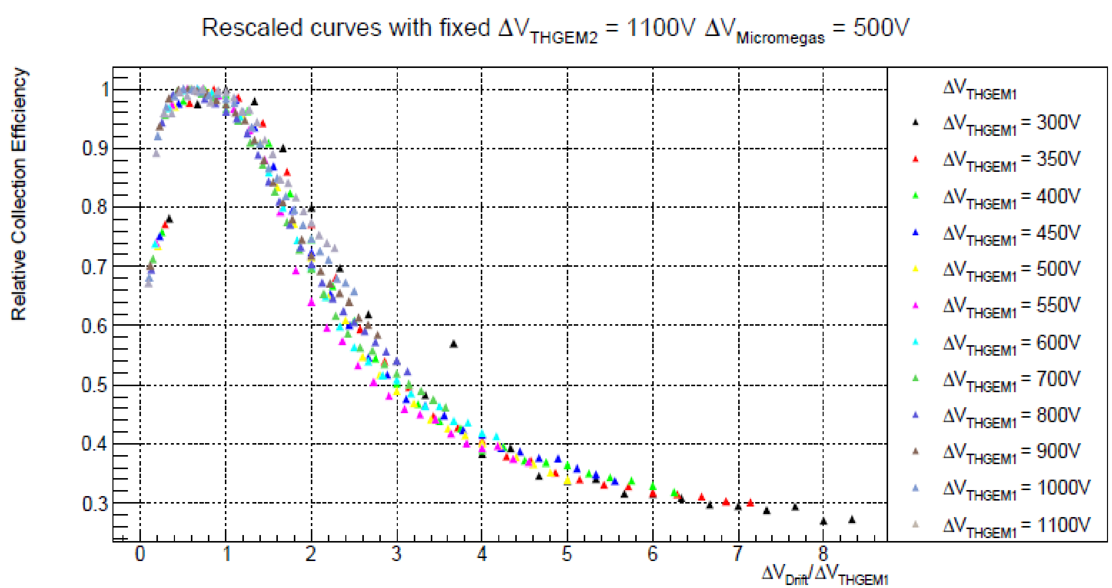

Transfer efficiency study

The behaviour of the Transfer Efficiency is different:

Saturating above 1 kV/cm

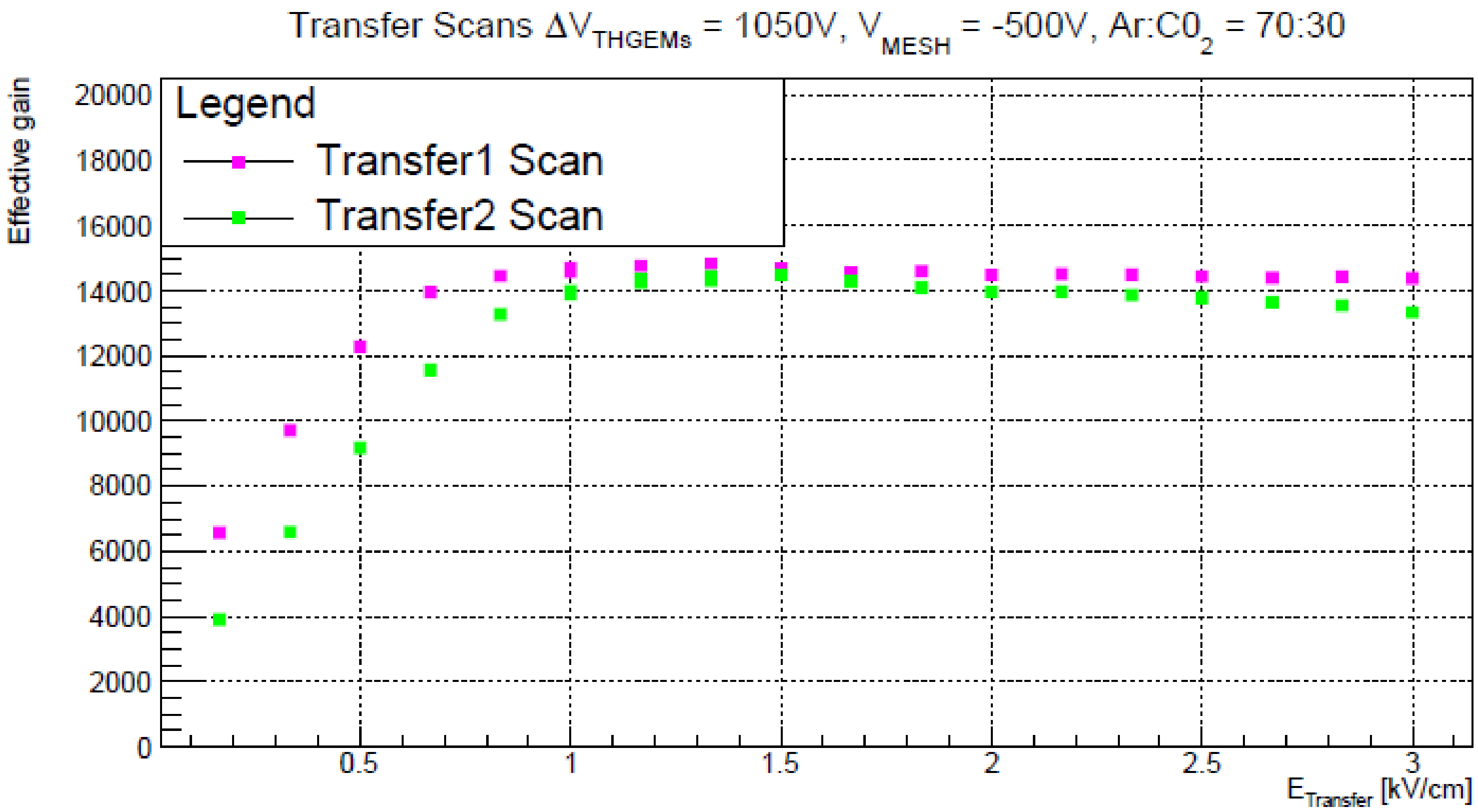

Normalized Gain Curve at fixed Collection Efficiency

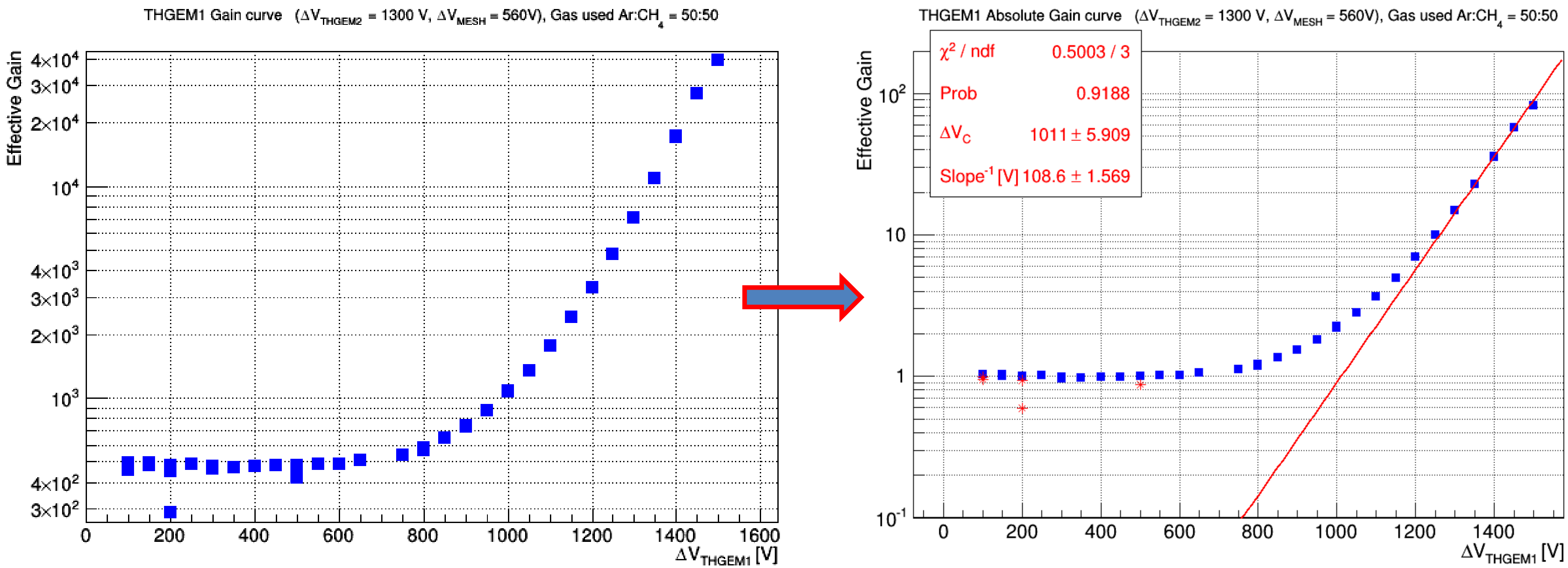

Fitting with the function $G = e^{\frac{(\Delta V_{THGEM1} - \Delta V_C)}{slope^{-1}}}$
where:

- ΔV_C critical voltage of THGEM1
- $slope^{-1}$ inverse of the slope of the exponential

For the last parameter, it is common to compute the voltage difference needed in order to obatin a variation in gain of an order of magnitude: $\Delta V_{10} = slope^{-1} \cdot ln(10)$.

Comparing Gain variations from single THGEM gain curves with the combined gain curve

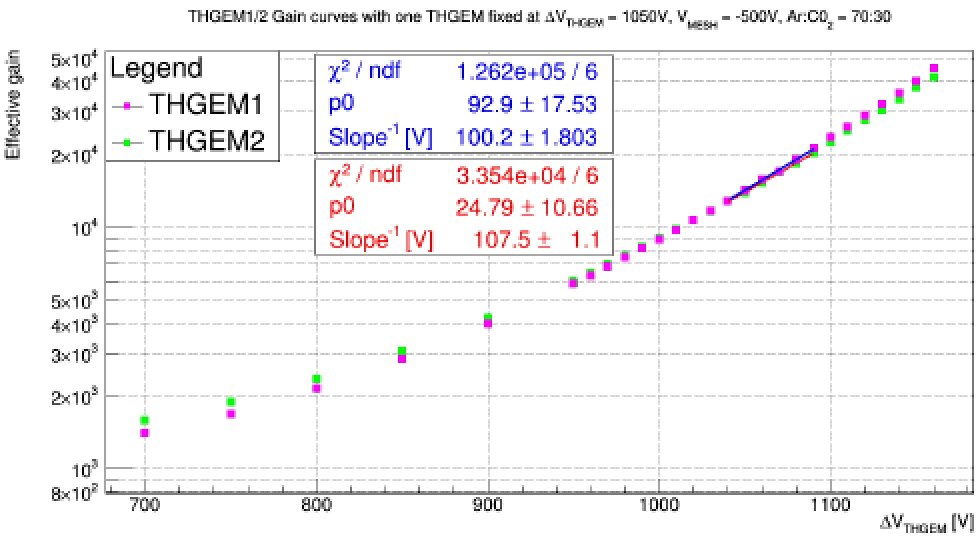

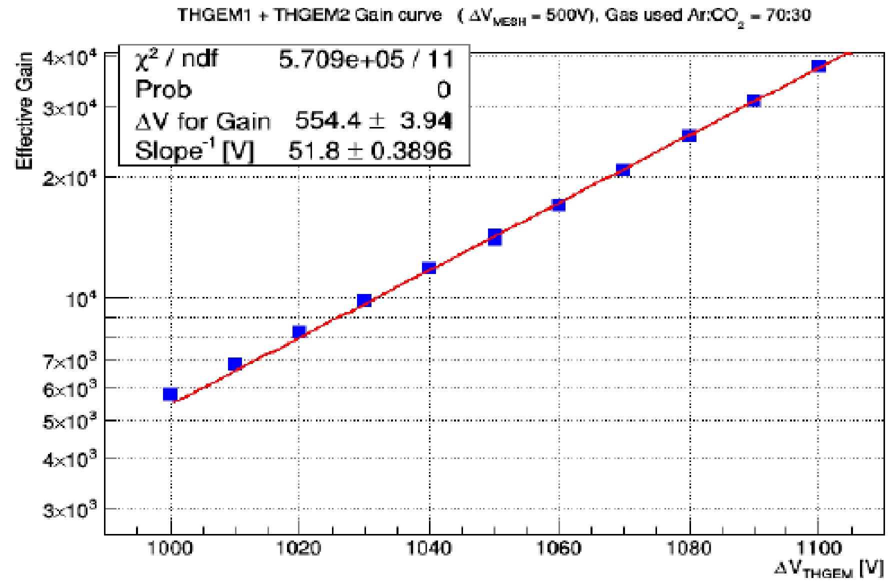

	THGEM1	THGEM2
$\Delta V_{10}[V]$	230.7 ± 4.2	247.5 ± 2.5

Estimated

$\Delta V_{10}^{THGEM1+THGEM2} = 119.5$ V

Measured

$\Delta V_{10}^{THGEM1+THGEM2} = 119.3 \pm 0.9$ V

Final values of the individual contributions

The Micromegas gain parameters could be determined as well.

All the parameters are now known for the 2 gas mixtures used.

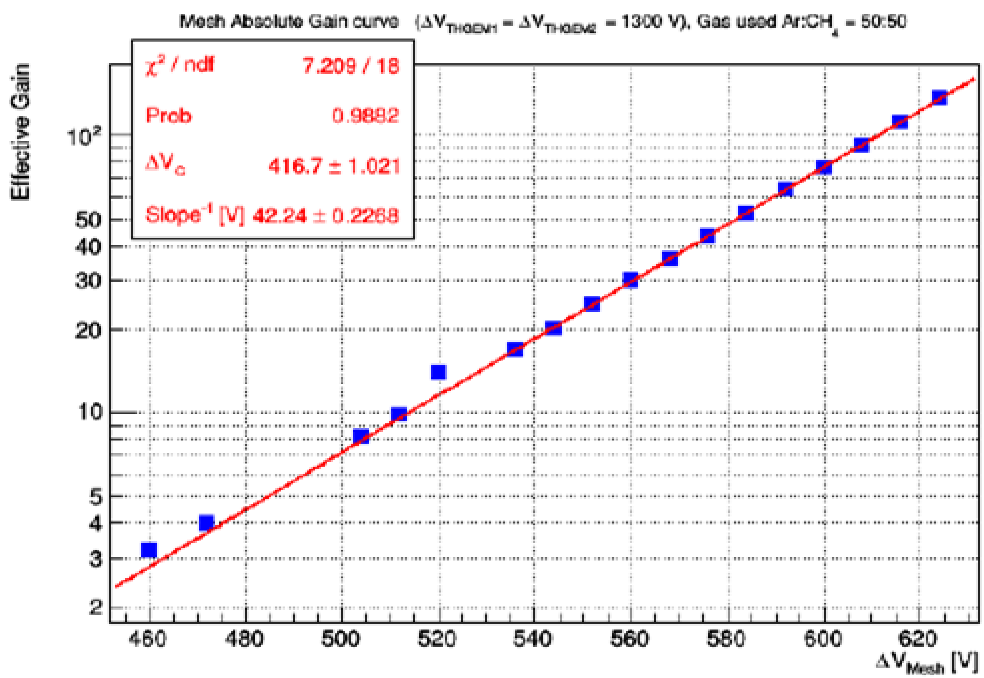

Summary of the measured parameters:

Gas mixture	ΔV_{10}^{THGEM1} [V]	ΔV_{10}^{THGEM2} [V]	ΔV_{C}^{THGEM} [V]	ΔV_{10}^{Mesh} [V]	V_{C}^{Mesh} [V]
Ar:C0$_2$ 70:30	230.7 ± 4.2	247.5 ± 2.5	847.6 ± 6.3	90.5 ± 0.3	322.1 ± 0.5
Ar:CH$_4$ 50:50	292.4 ± 3.6	324.7 ± 5.4	1011.0 ± 5.9	97.3 ± 0.5	416.7 ± 2.3

Gain Sharing between the two THGEMs in Ar:CO_2 70:30

Using the measured parameters it was possible to estimate the Effective gain values given by the sharing between THGEM1 and THGEM2 (blue points).
Excellent agreement between the measured and the expected values!

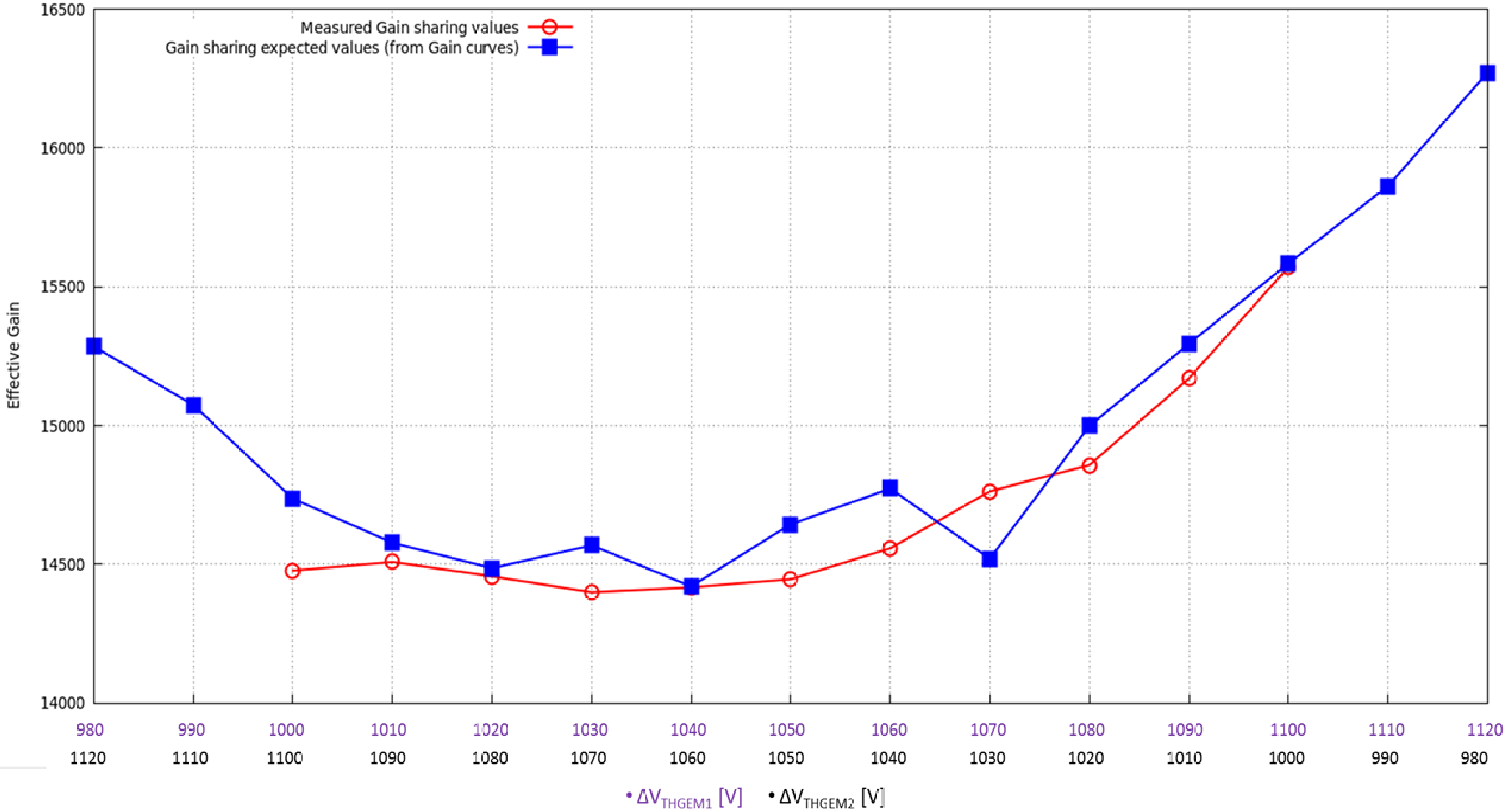

Gain – Pressure dependence

The gain of a gaseous detector depends on the gas temperature and pressure.

The knowledge of this dependence is fundamental for a stable operation!

Goal: obtain the factor useful to provide an automatic compensation of the pressure induced gain variations

(the temperature induced variations are negligible in time scale with respect to pressure induced ones)

Pressure dependence

Dependence of the gain on the pressure:

$$G = G_0 \cdot e^{-K(P-P_0)}$$

where

- G_0 gain at pressure $P = P_0$
- $K = slope^{-1}$ constant depending on the gas mixture and other variables

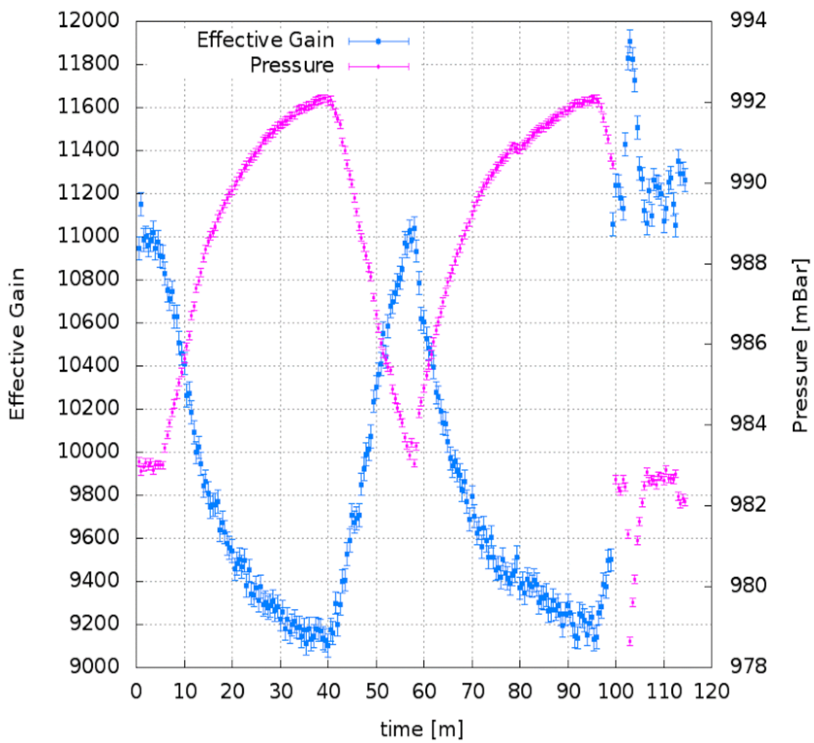

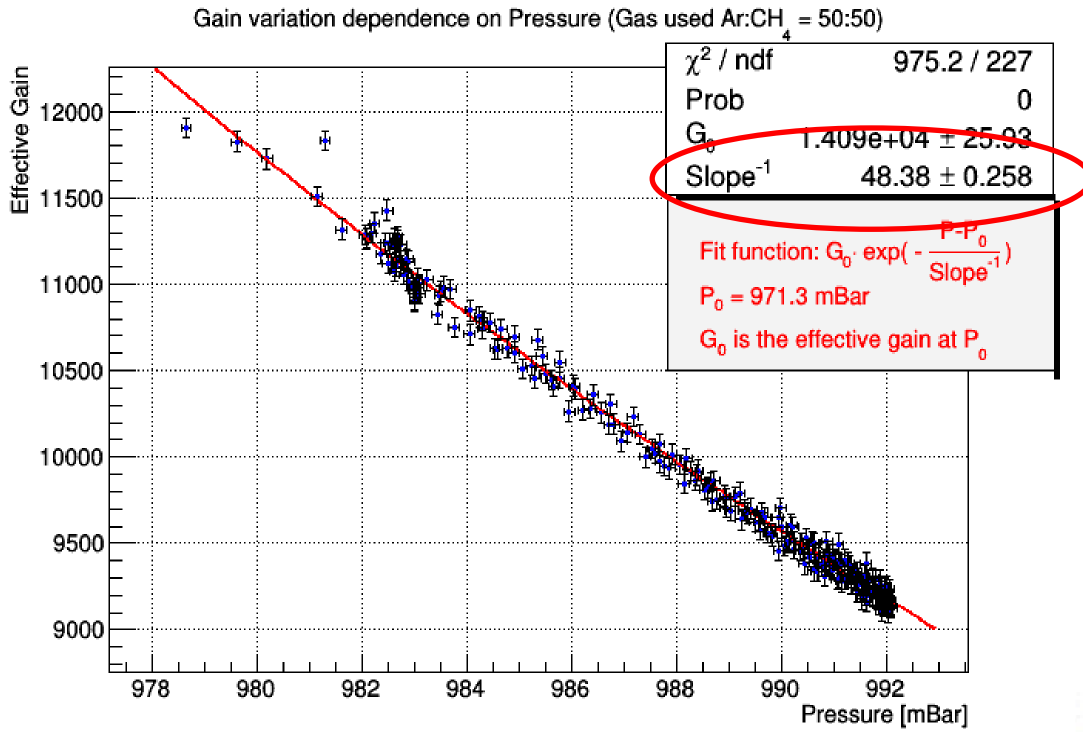

Ion BackFlow studies

Experimental setup used:

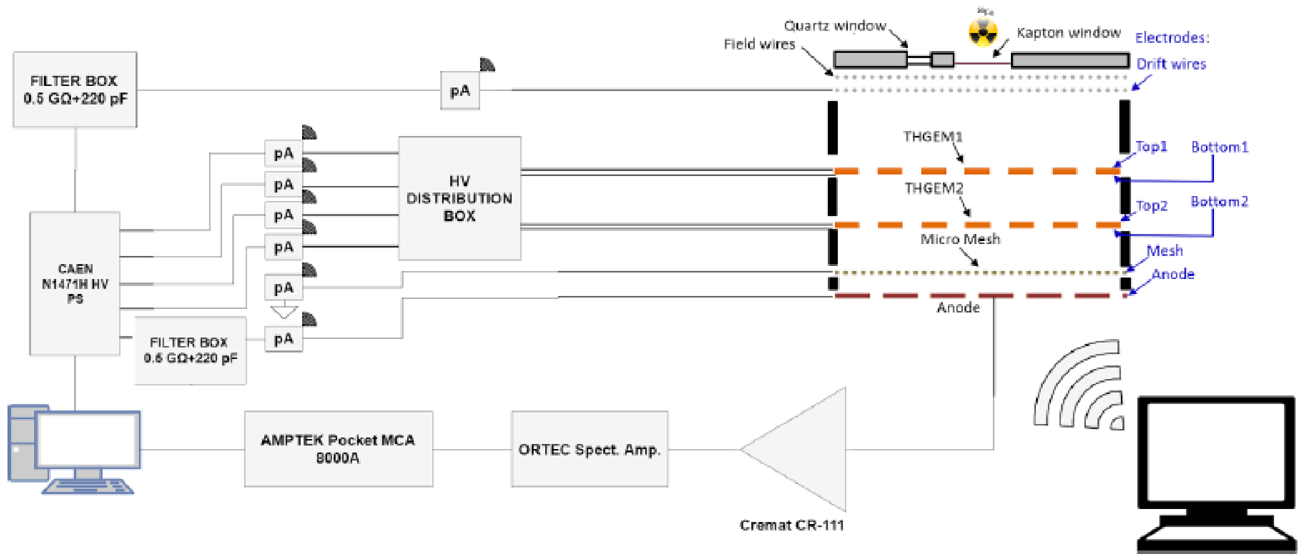

In literature the definition is not unique.
I choose to normalize all currents with respect to the anodic current, roughly:

$$I_{anode} \simeq n_p \cdot G_{eff} \cdot R$$

being:

- $n_p \sim 2 \cdot 10^2$
- $R \sim 1kHz$
- $G_{eff} \sim O(10^4)$

thus $I_{anode} \sim$ few 10^2 pA.

Home-made Picoammeters

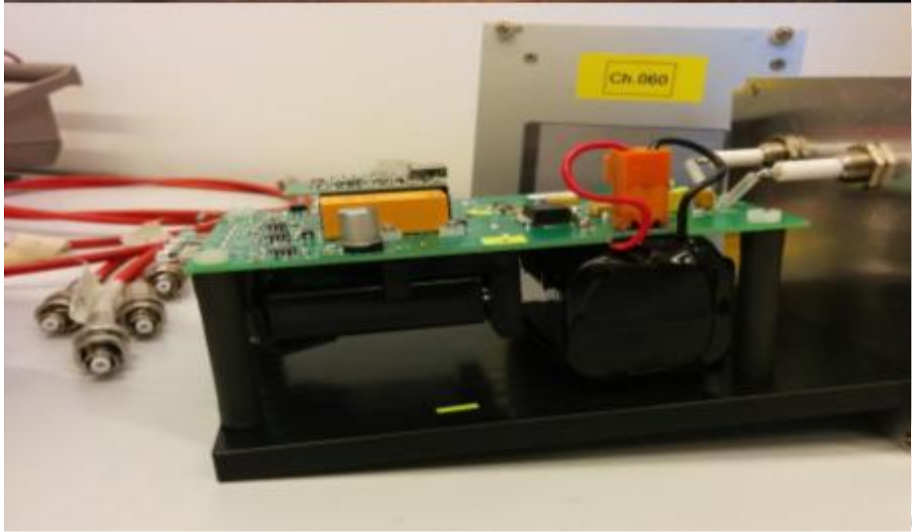

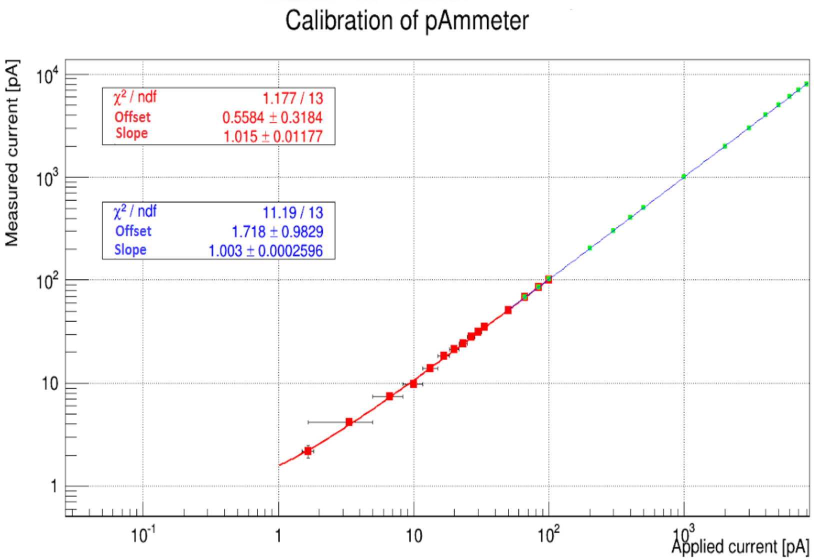

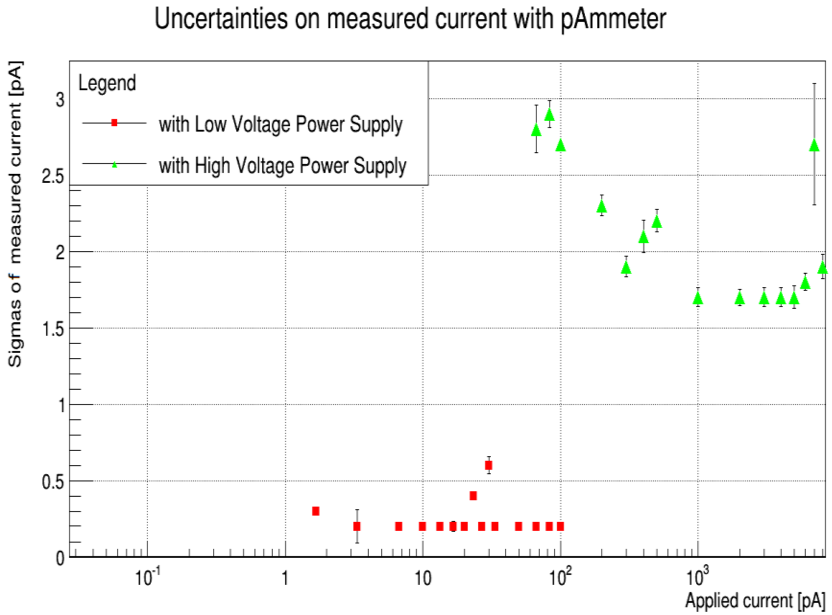

Currents on the seven electrodes

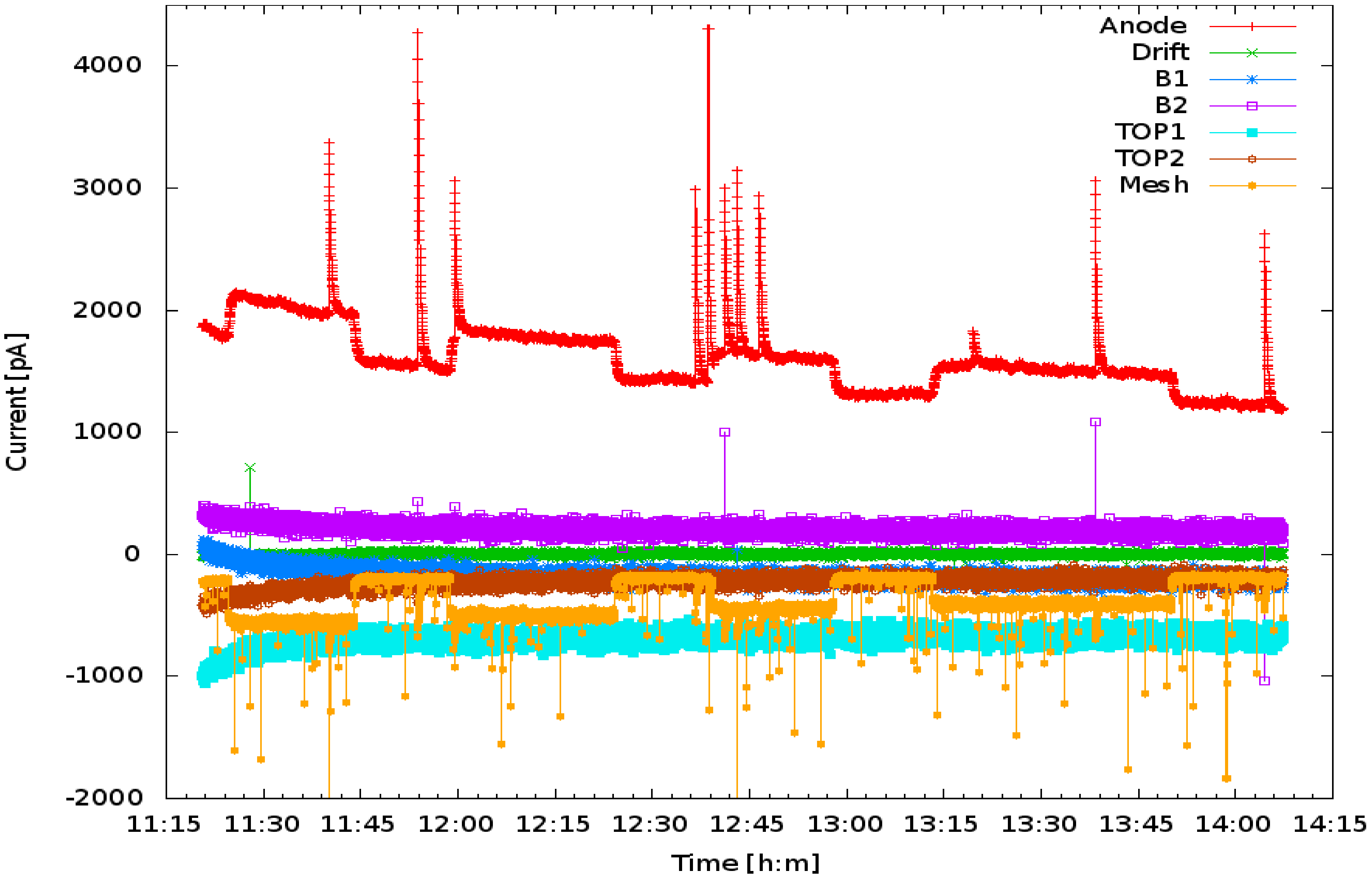

Baseline Subtraction on the Anodic Current

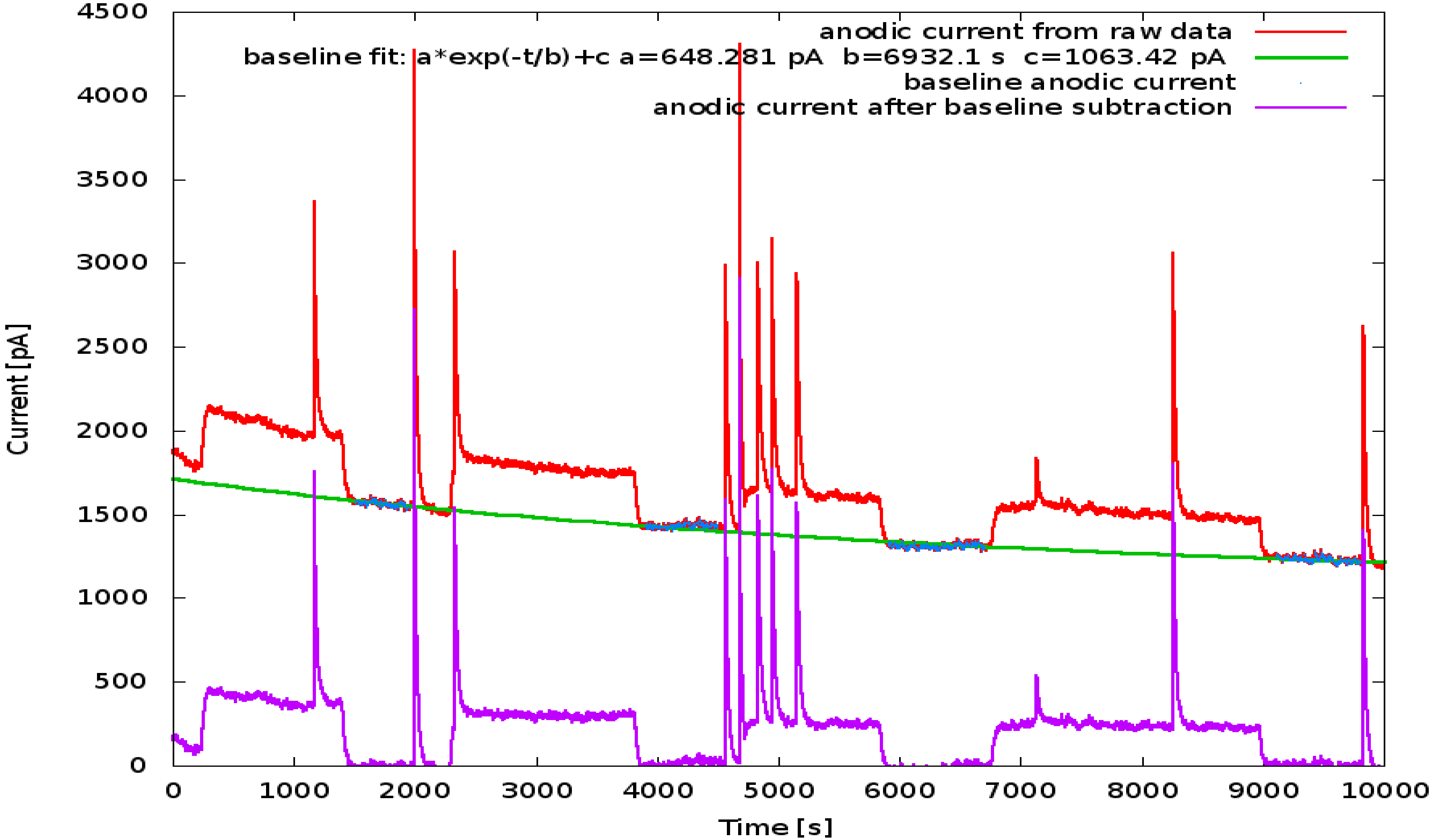

Micro-discharge correction

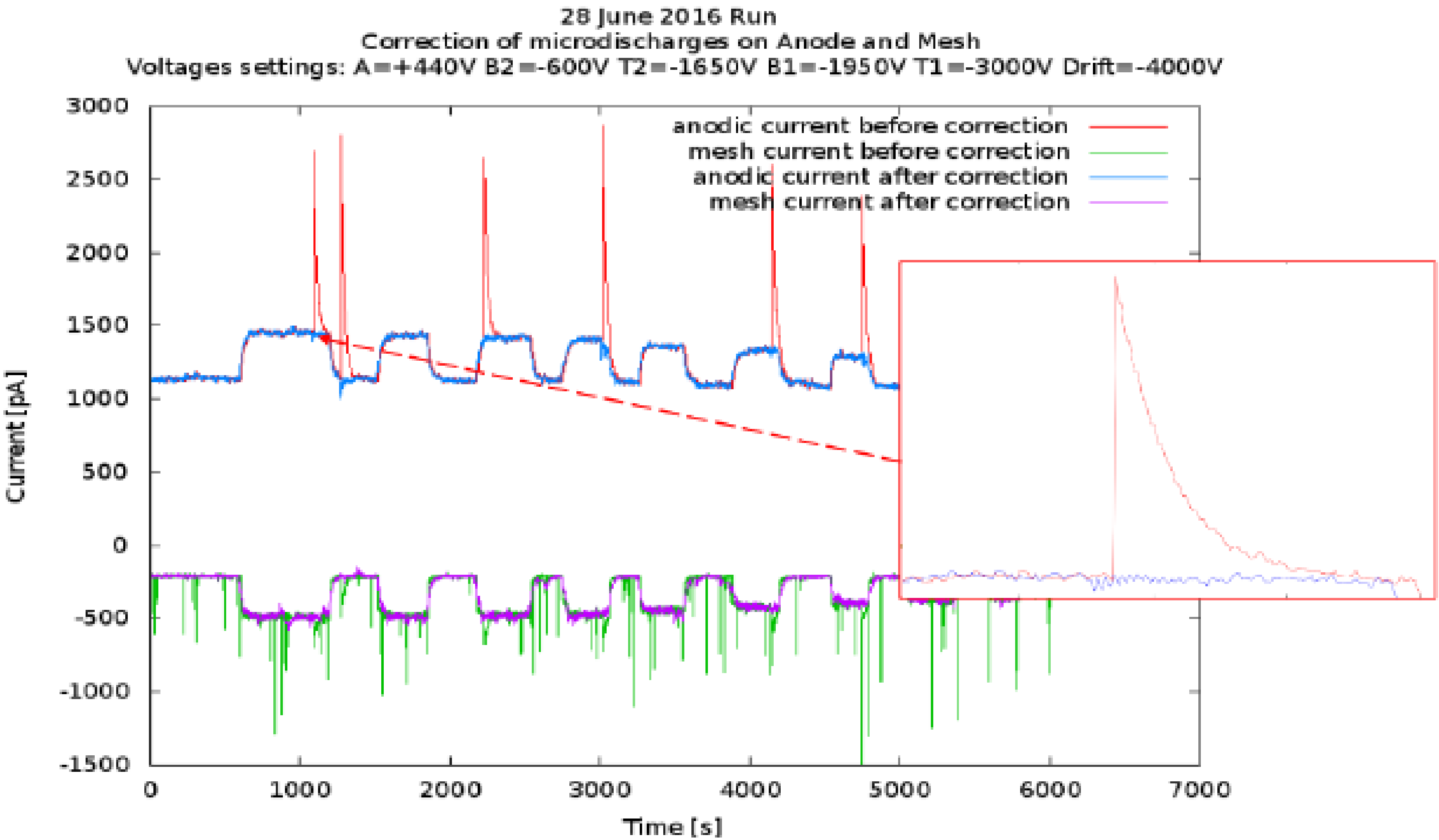

Quality Check

The chamber is a closed system $\Rightarrow \sum_{i=electrode}^{7} < I_{electrode} > \approx 0$ in each time interval.
Measurements not satisfying this requirement within 3 σ error were rejected.

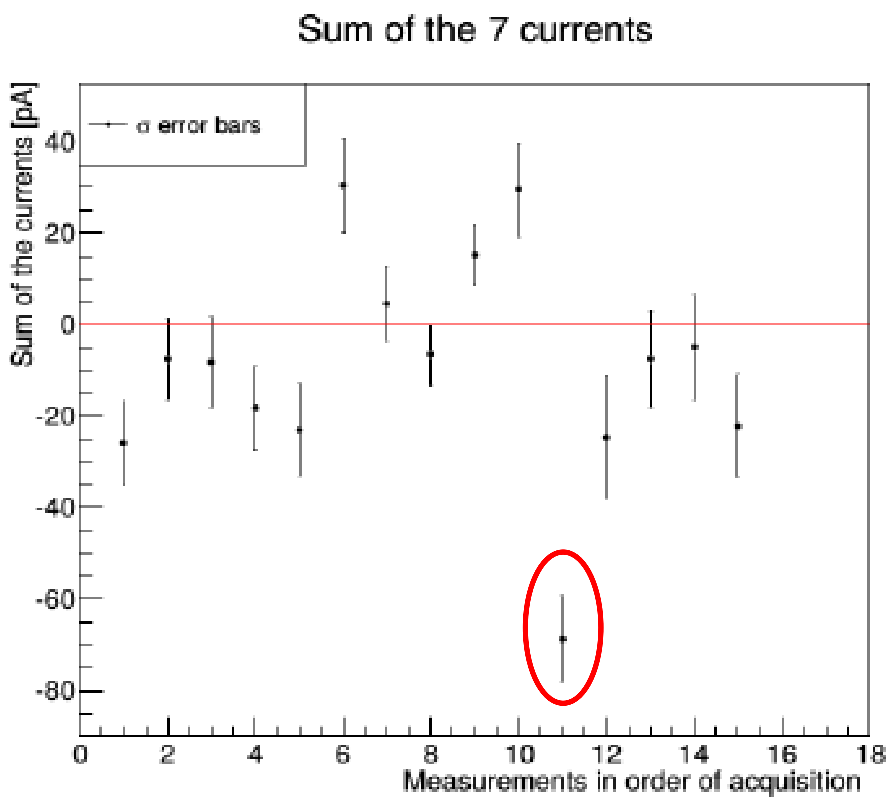

Micromesh: an excellent Ion Trap!

~ 90% of ions are captured by it

(excellent agreement with the literature for $\xi = 18$)

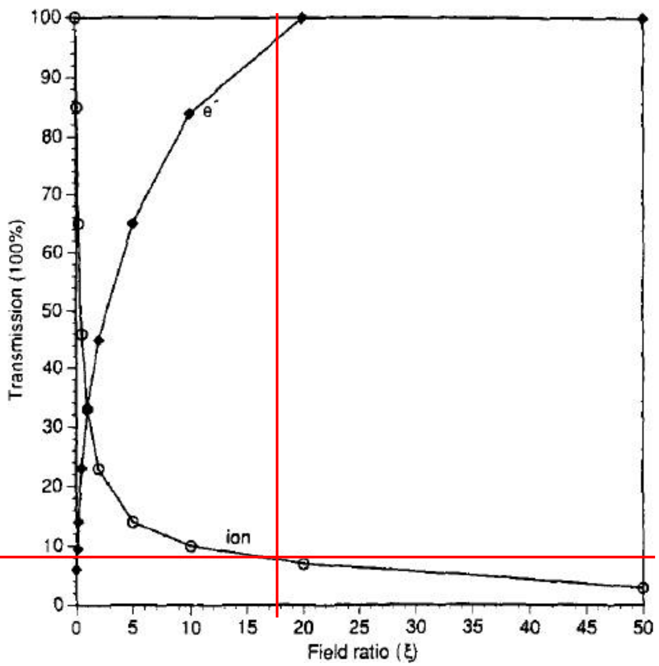

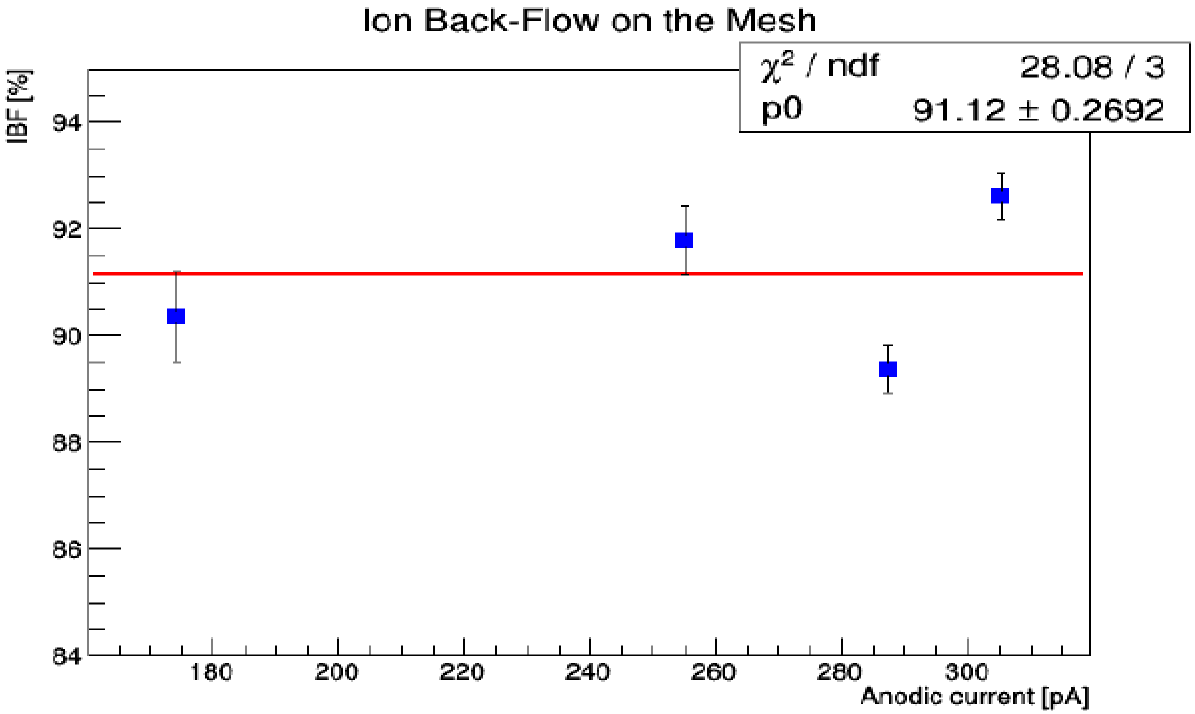

First results

Total IBF in the drift region: less than 5%.

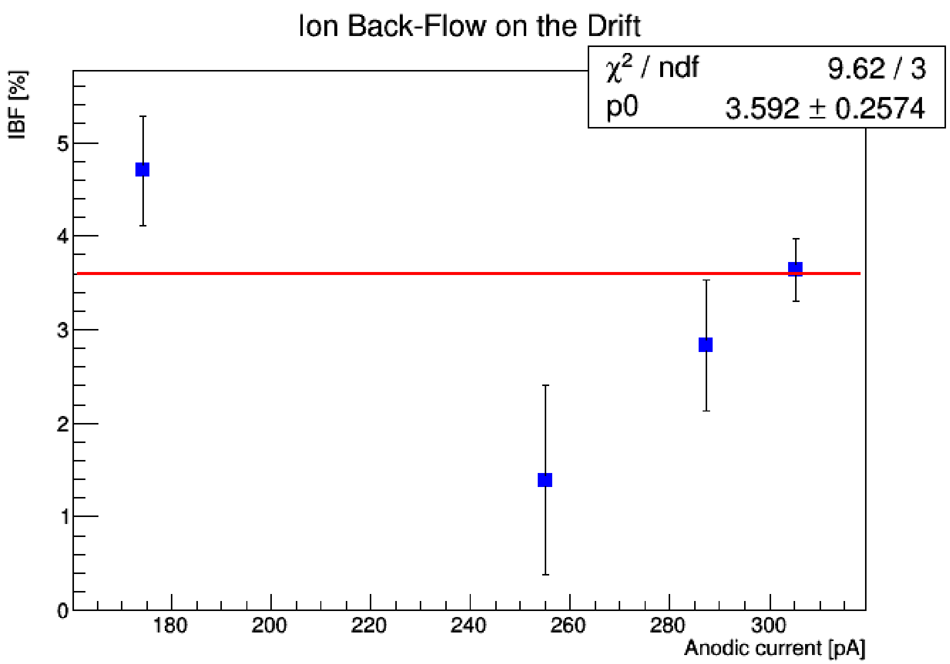

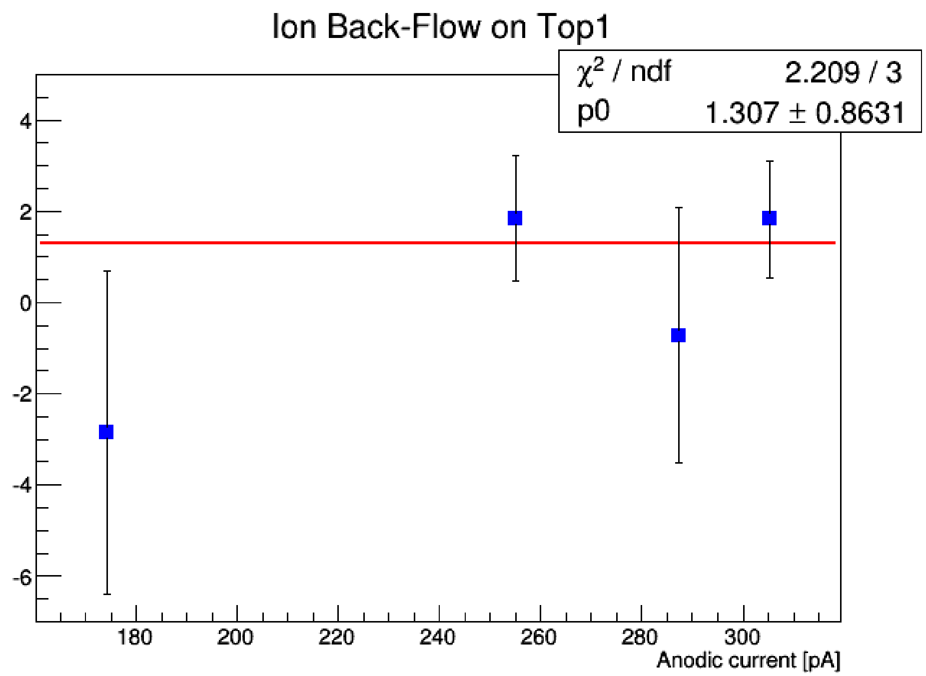

IBF dependence on the Drift field

IBF sharing between

the Top1 and Drift:

The total IBF in the drift region

remains contant.

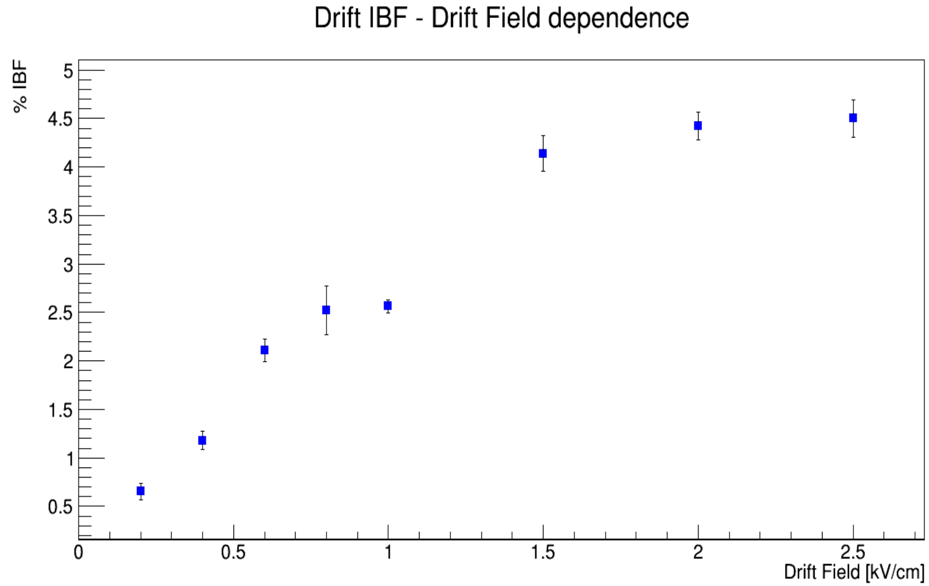

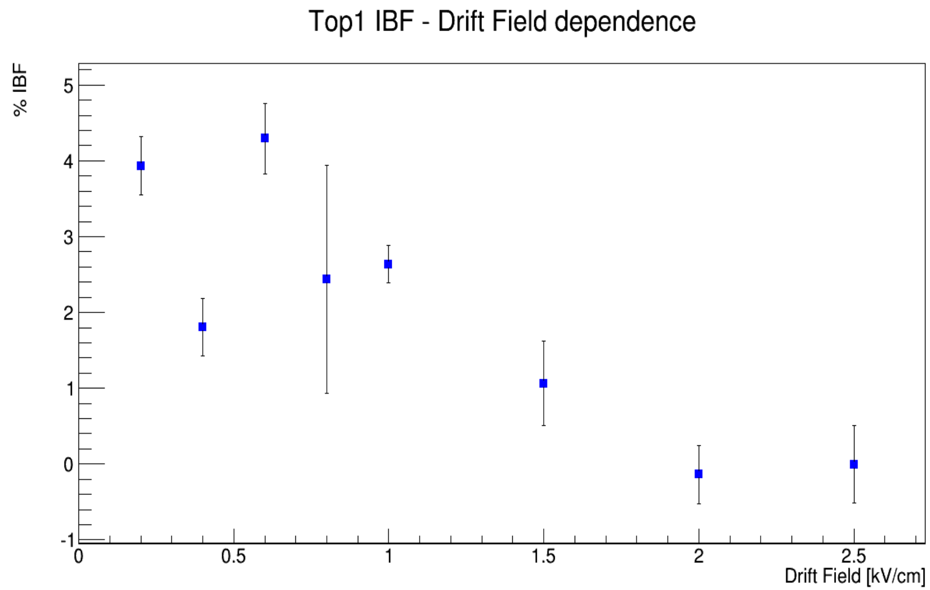

IBF dependence on the Transfer1 field

The total IBF in the drift region remains contant around 5%. Small decreasing trend on the Drift with respect to $E_{Transfer1}$

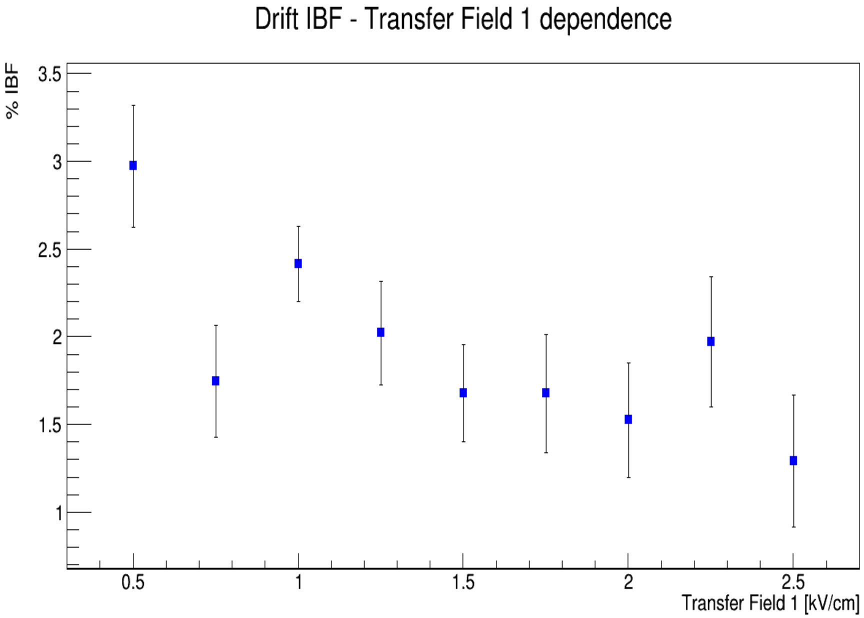

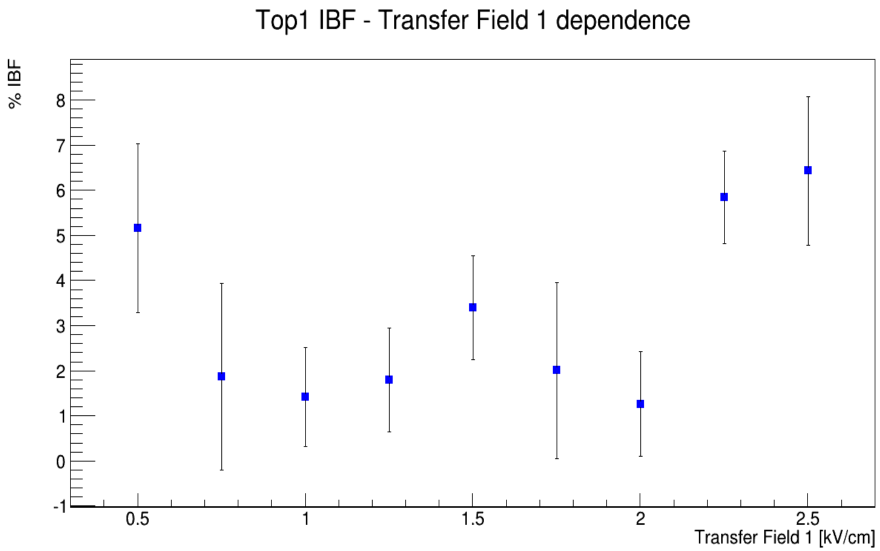

IBF dependence on the Transfer2 field

IBF on Top1 and on the Drift does not depend on $E_{Transfer2}$ (as expected!)

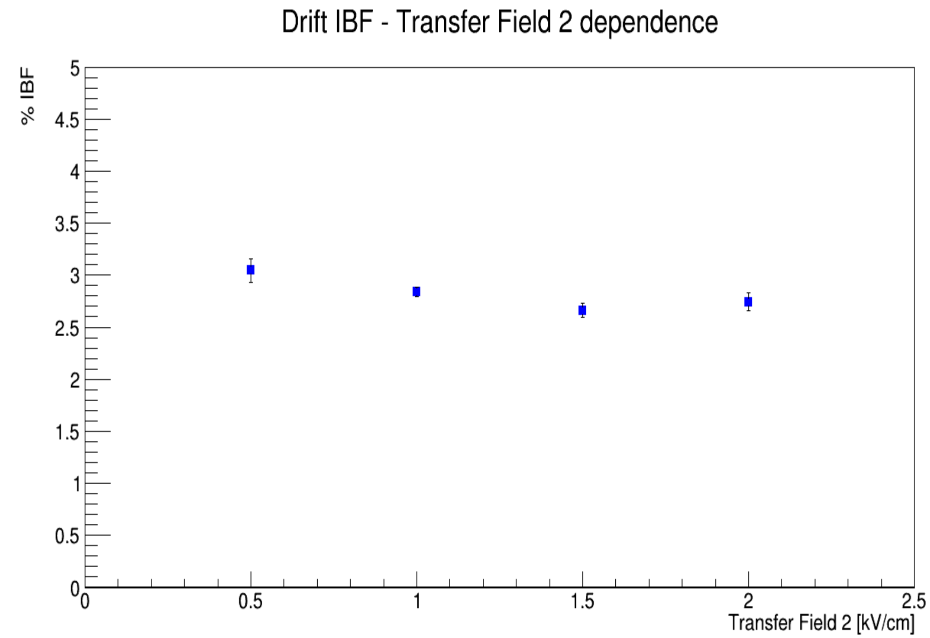

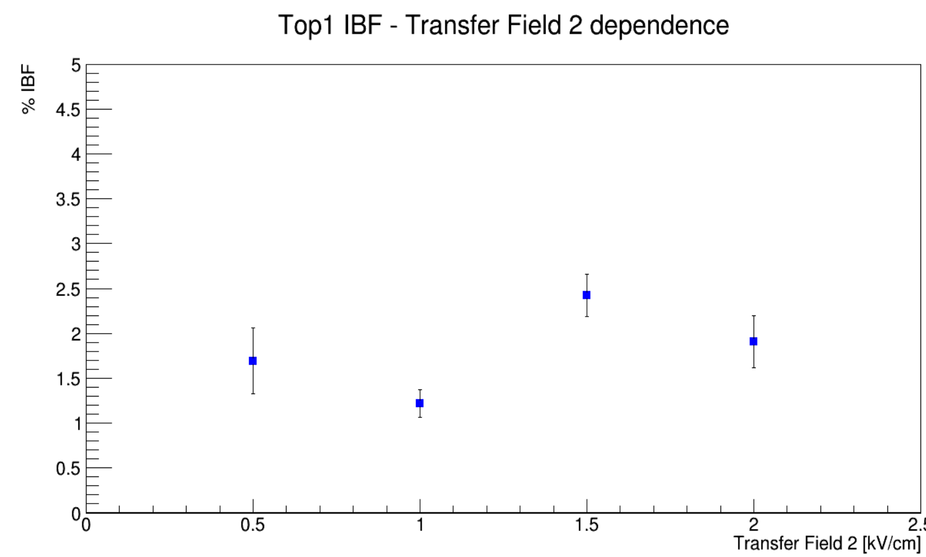

IBF dependence on the Transfer2 field

IBF sharing between the Botton2 and Mesh

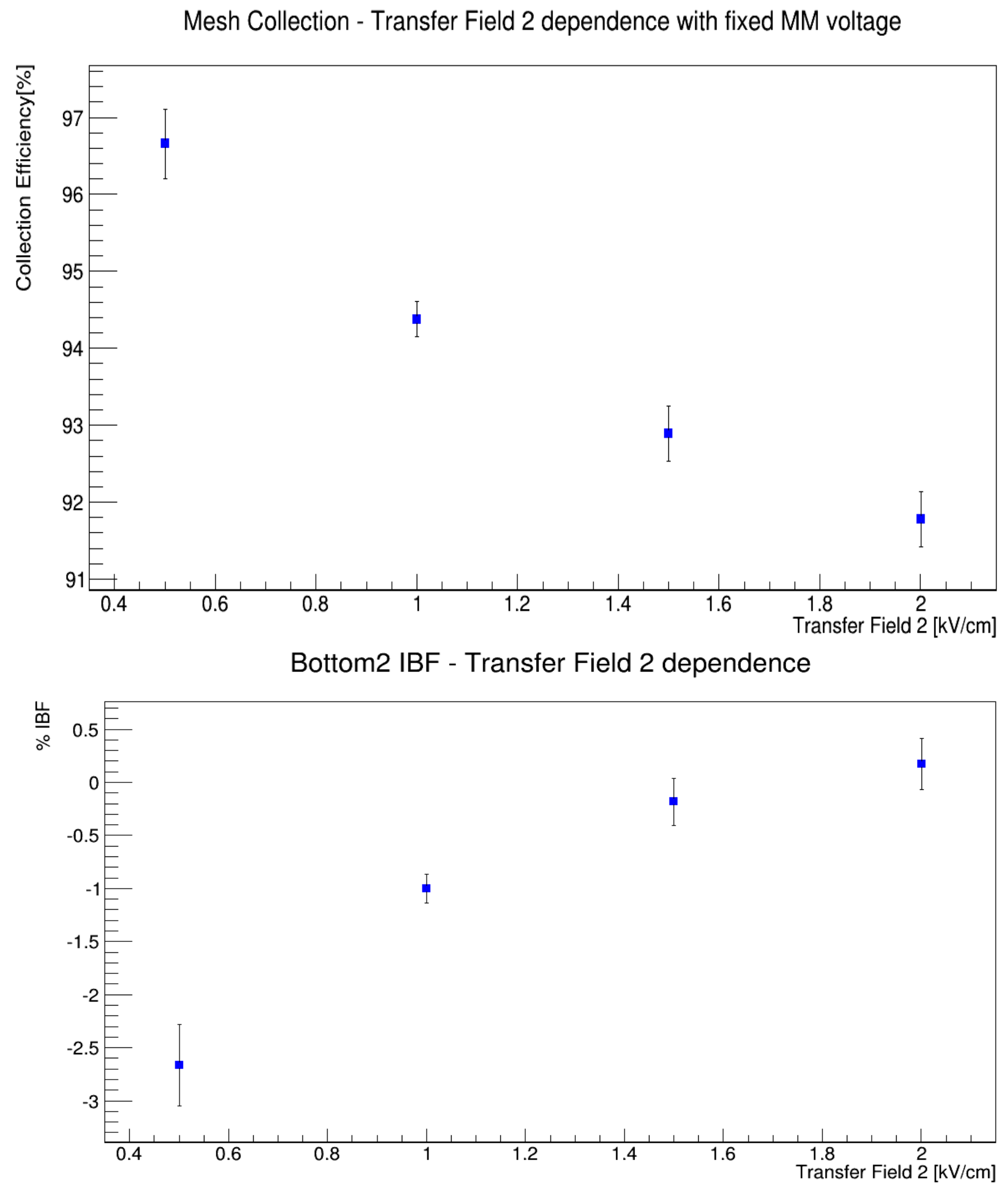

IBF in COMPASS RICH-1 conditions using ^{55}Fe source

Gas used: Ar/CH4 50/50

Same voltage settings of COMPASS RICH-1 apart ΔV_{drift} =800V

Total IBF in the drift region: less than 3%.

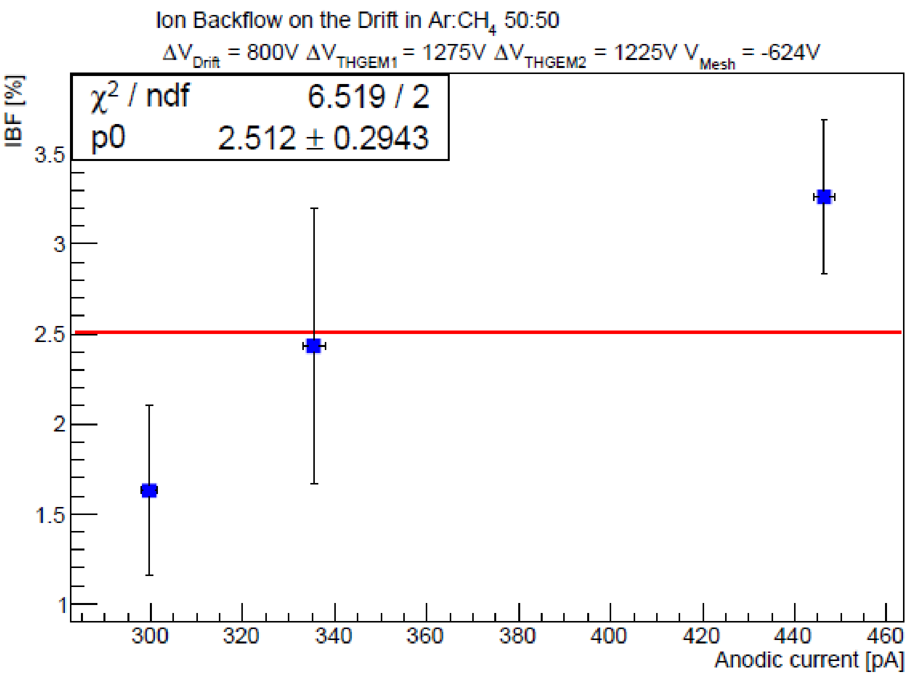

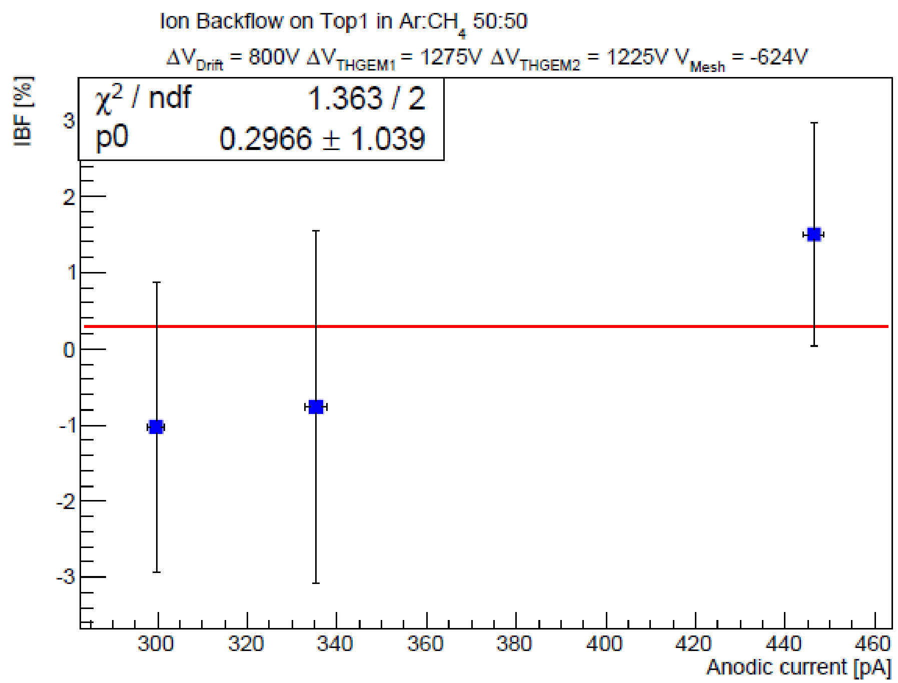

IBF in COMPASS RICH-1 conditions using UV source

Gas used: Ar/CH4 50/50

Same voltage settings

(apart $\Delta V_{drift} = 0V$)

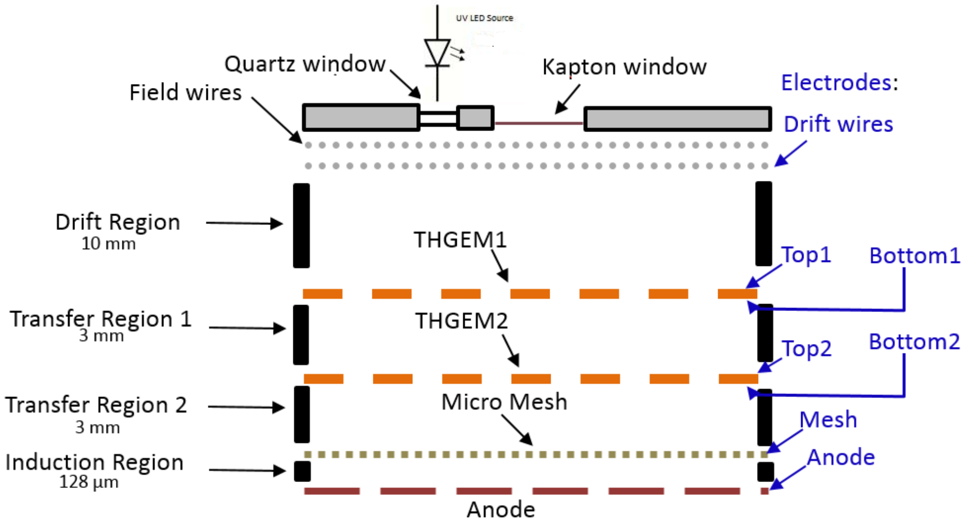

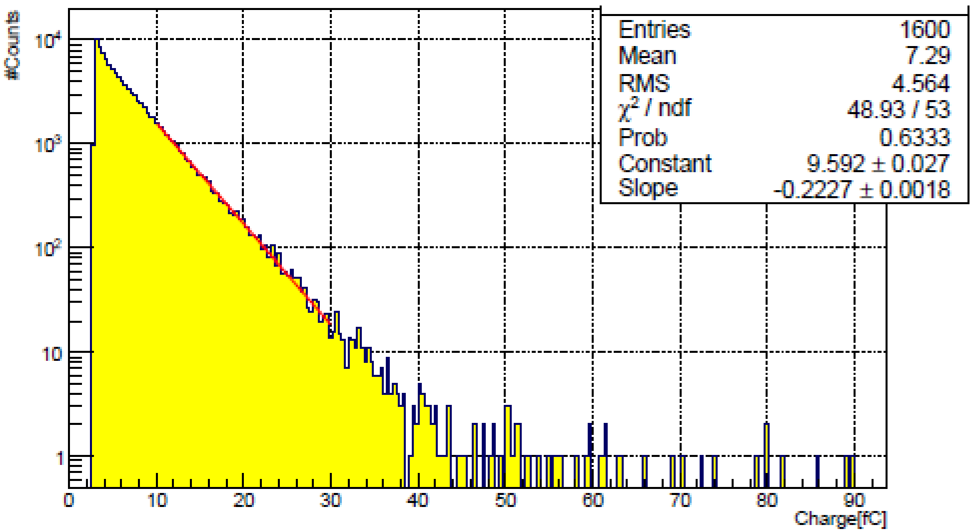

IBF in COMPASS RICH-1 conditions using UV source

Excellent ion-blocking efficiency of the mesh: 96.5 ± 0.1 %

$\xi \sim 80\% \rightarrow$ ion transparency $\leq 4\%$ from literature!

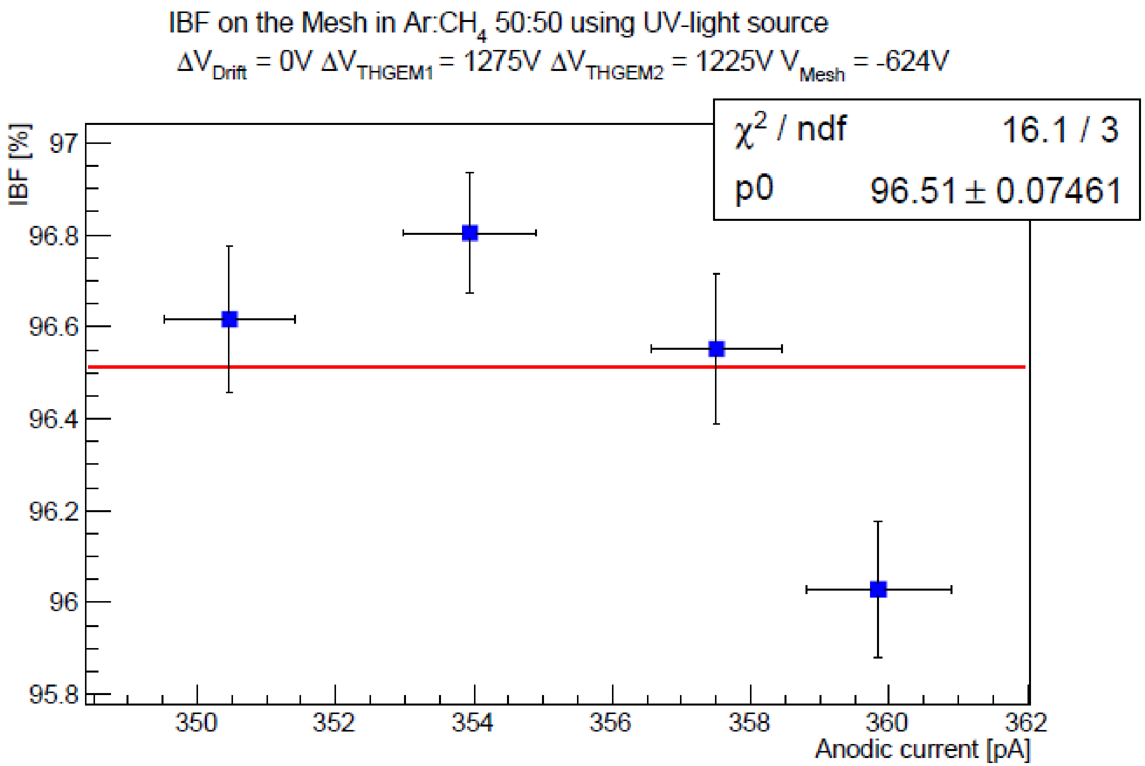

IBF in COMPASS RICH-1 conditions using UV source

IBF to the photocathode $\leq$ 3%

comparable with the total IBF in the drift region measured with ^{55}Fe source

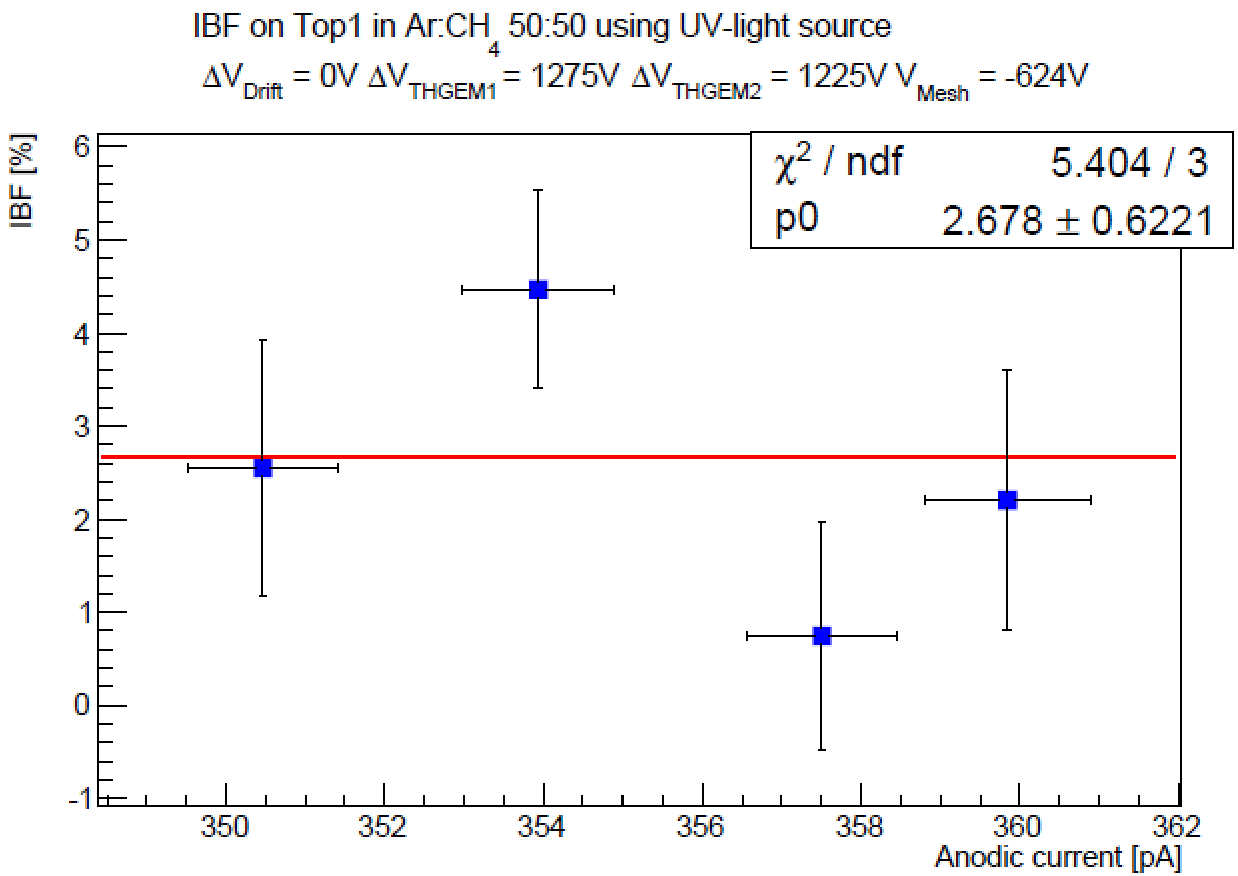

Conclusions

- **The present work contributes to the understanding of the performances of the novel MPGD-based Photon Detectors and their effectiveness in minimizing the aging of the CsI coated photocathode: IBF < 3%, which is a world record!**

- **Anyway in the future simulation studies and further measurements could be performed for a better understanding of the results obtained by me.**

THANK YOU ALL!





Conclusions

Concerning the Ion BackFlow measurements:

- I showed that using the high resolution picoammeters built at INFN Trieste, an accurate measurement of the IBF can be achieved
- The IBF dependence on the various electric fields in this new hybrid MPGD architecture has been studied
- The most important result of my work was to demonstrate that, in the electric field configuration used during the COMPASS RICH-1 operation, the fraction of IBF to the photocathode is below 3%.

BACKUP SLIDES

Gain Sharing between the THGEMs and Mesh in $Ar:CO_2$ 70:30

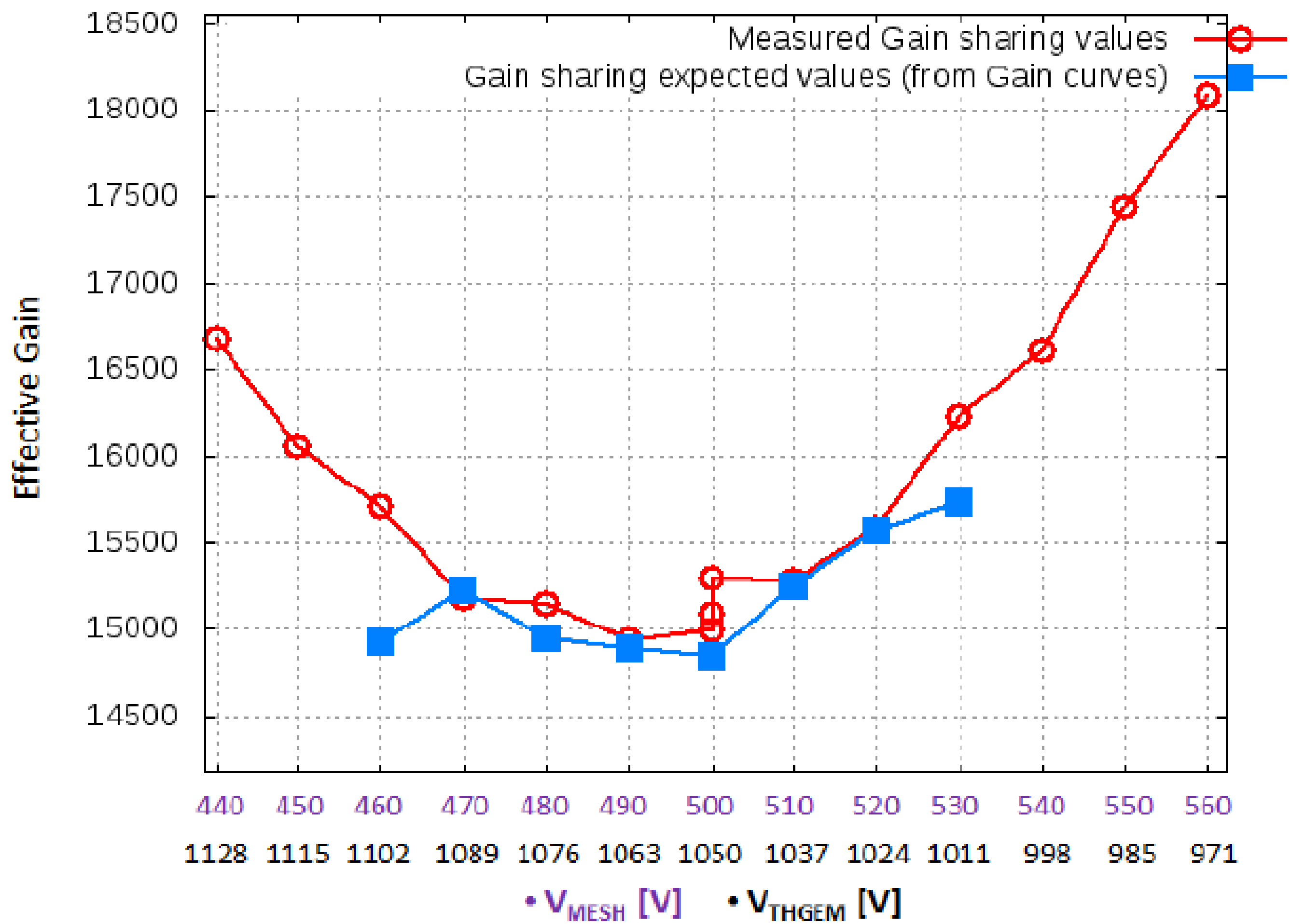

IBF in COMPASS RICH-1 conditions using UV source

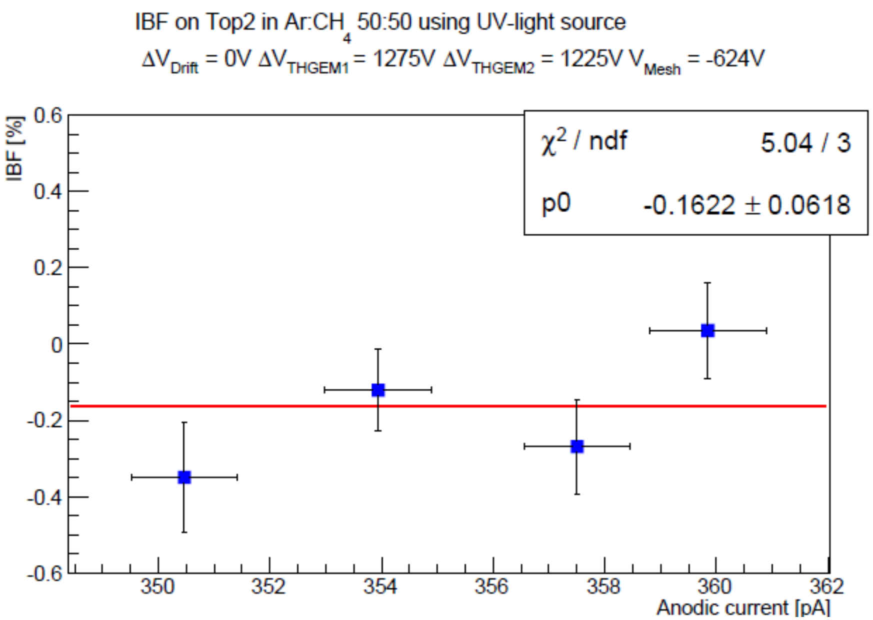

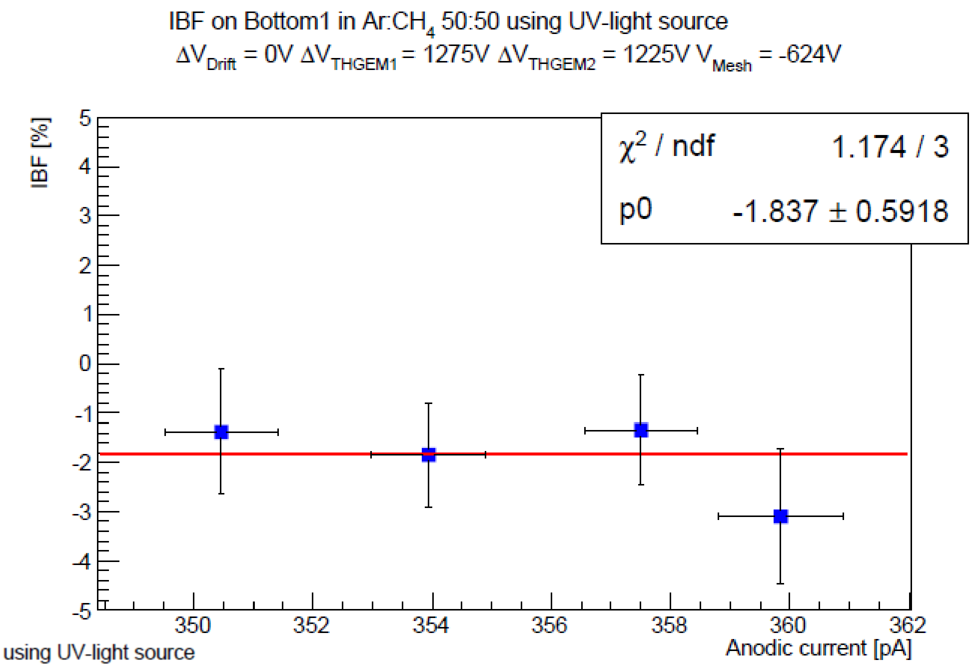

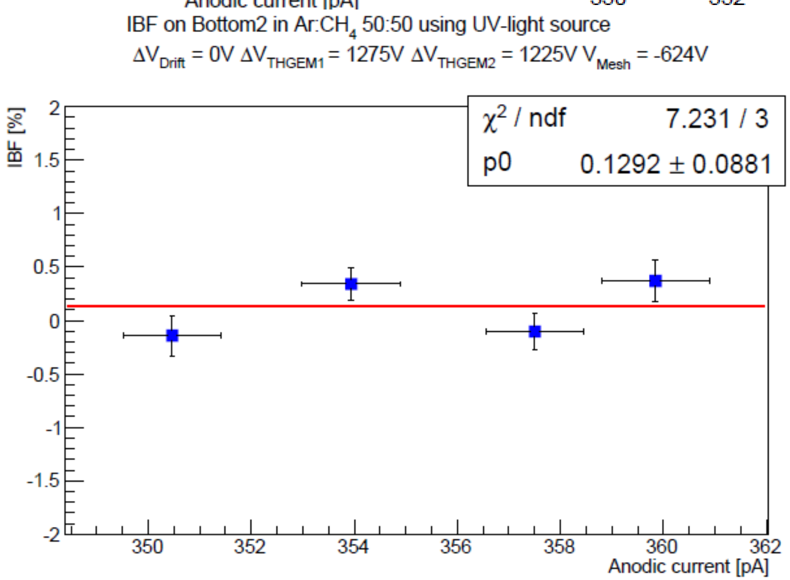

Ionization probability

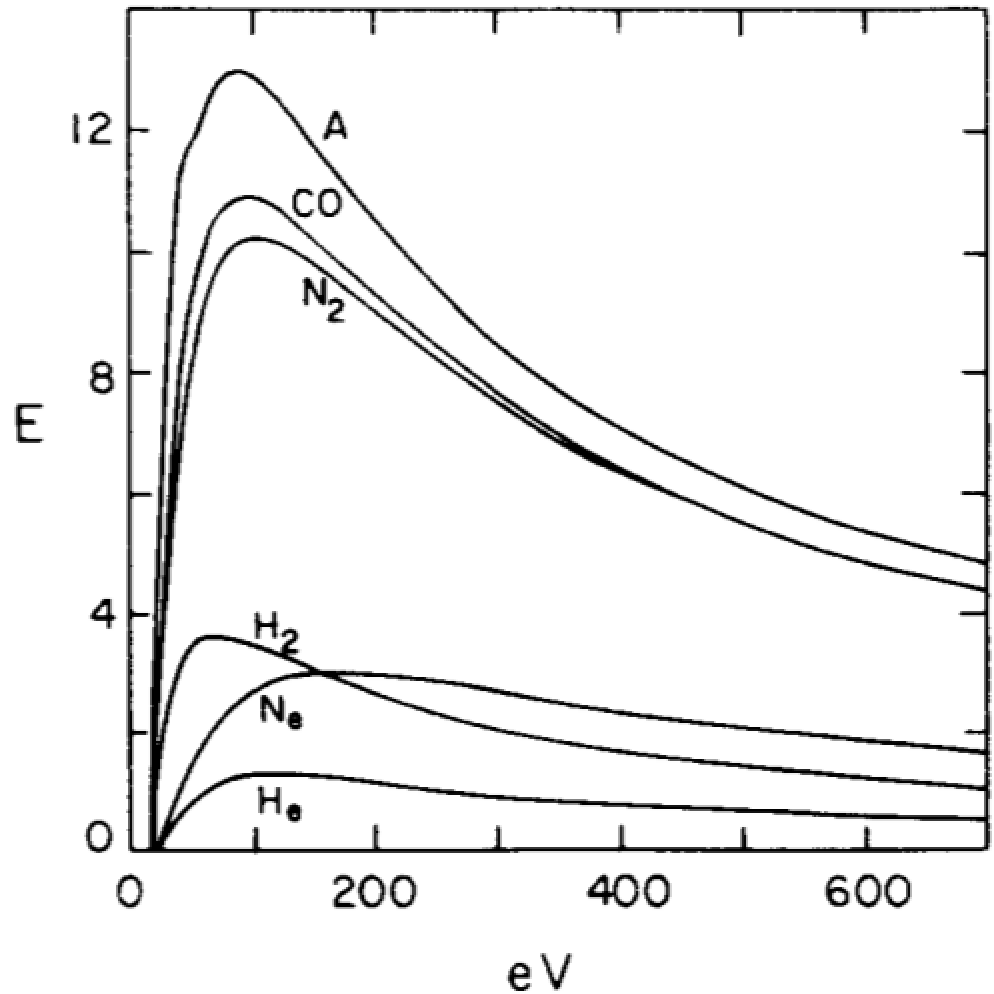

Ionization

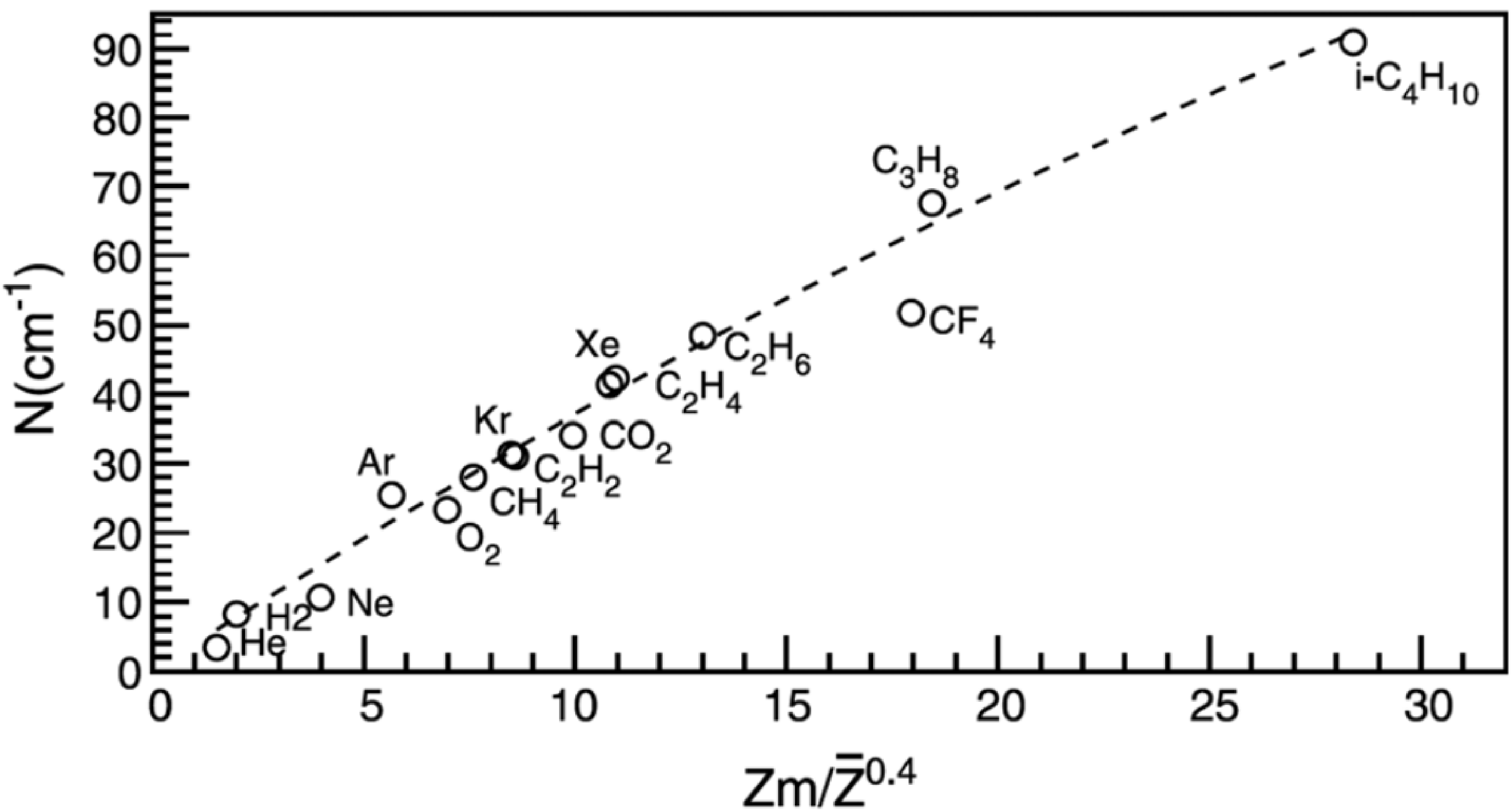

N(cm-1)
Zm/Z0.4
i-C4H10
C3H8
CF4
C2H6
C2H4
Xe
CO2
Kr
C2H2
Ar
CH4
O2
Ne
H2
He

CsI QE

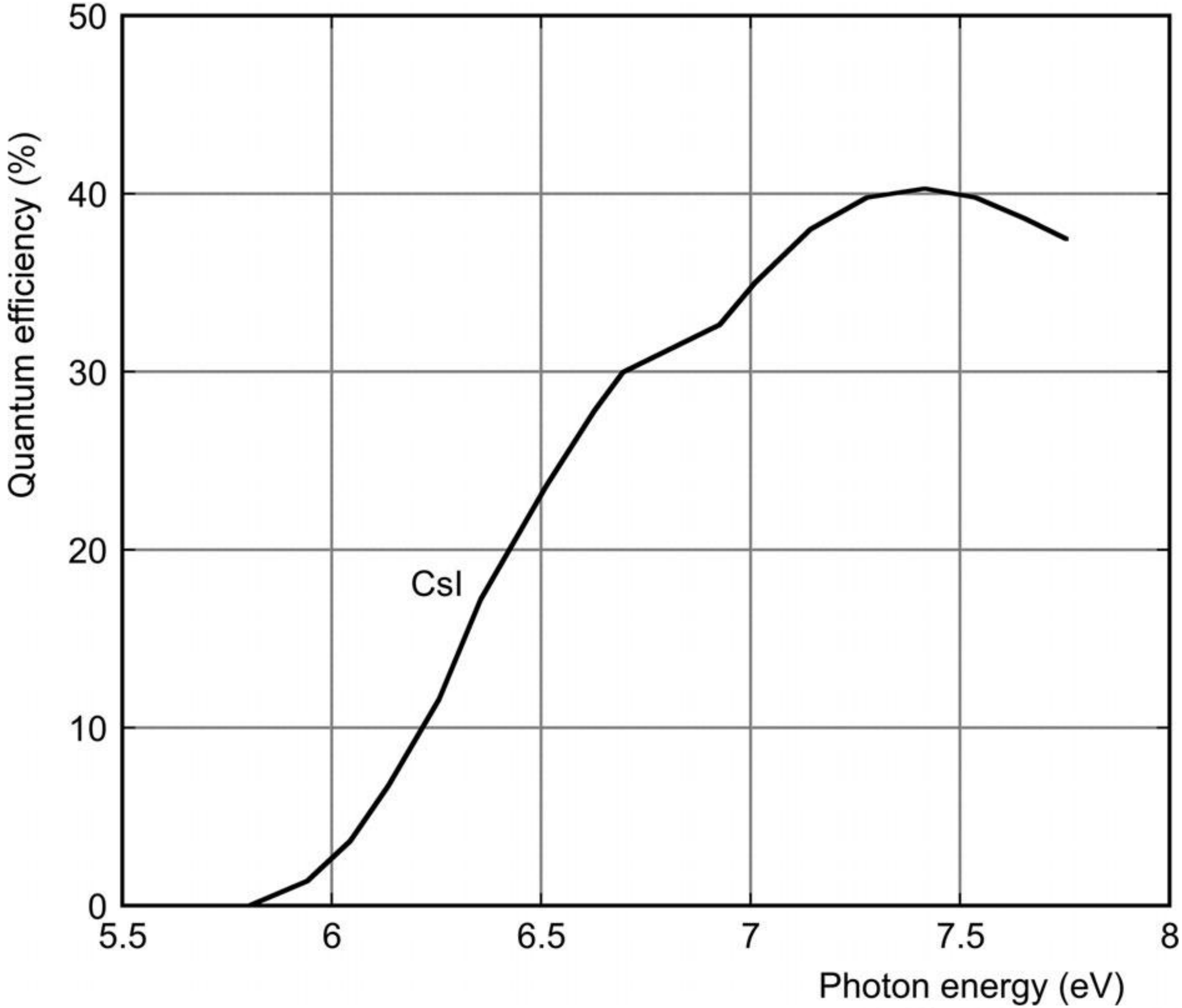
50
40
30
20
10
0
Quantum efficiency (%)
CsI
5.5
6
6.5
7
7.5
8
Photon energy (eV)

Extraction Efficiency

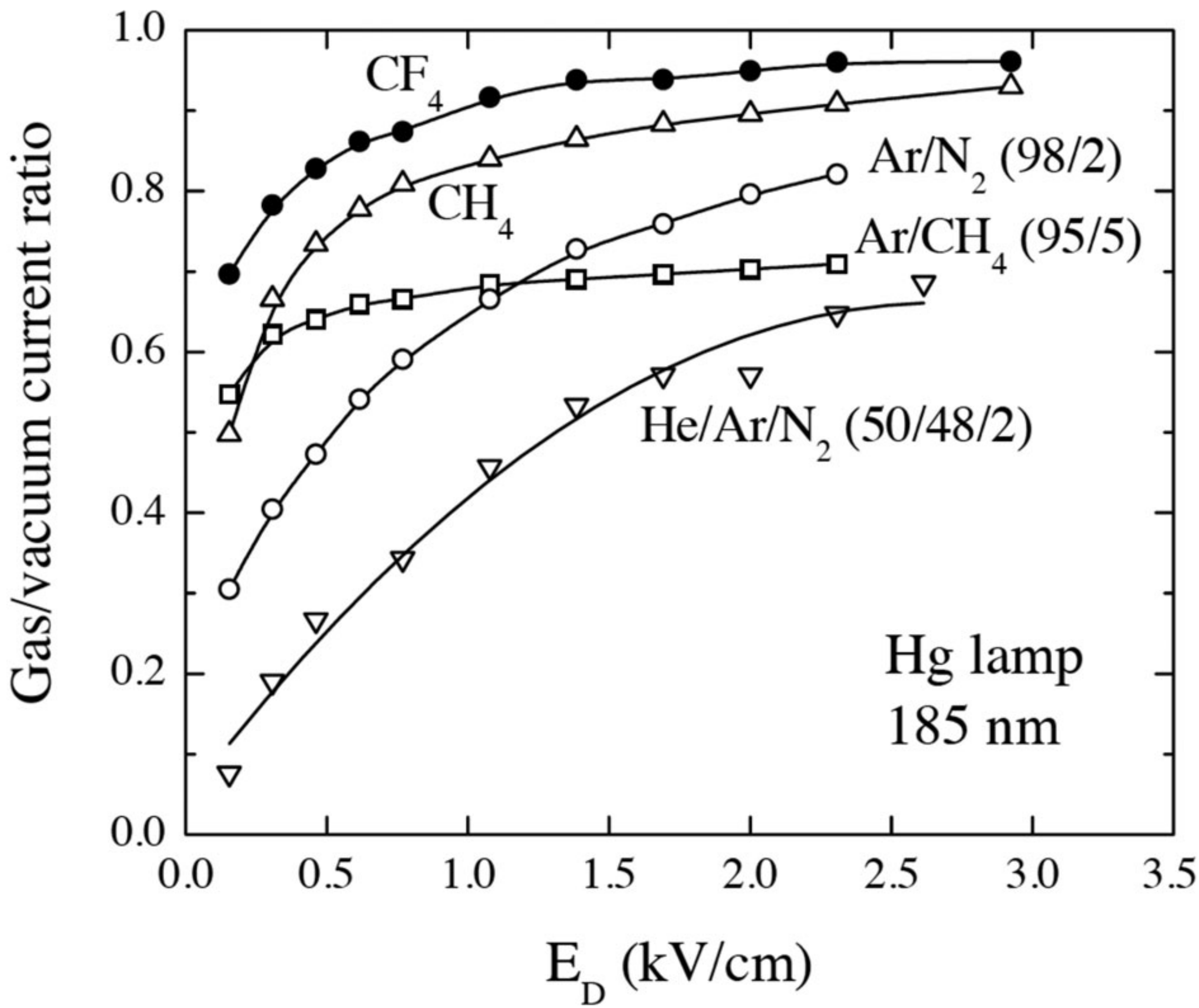

Rate Capability: GEM vs MWPC

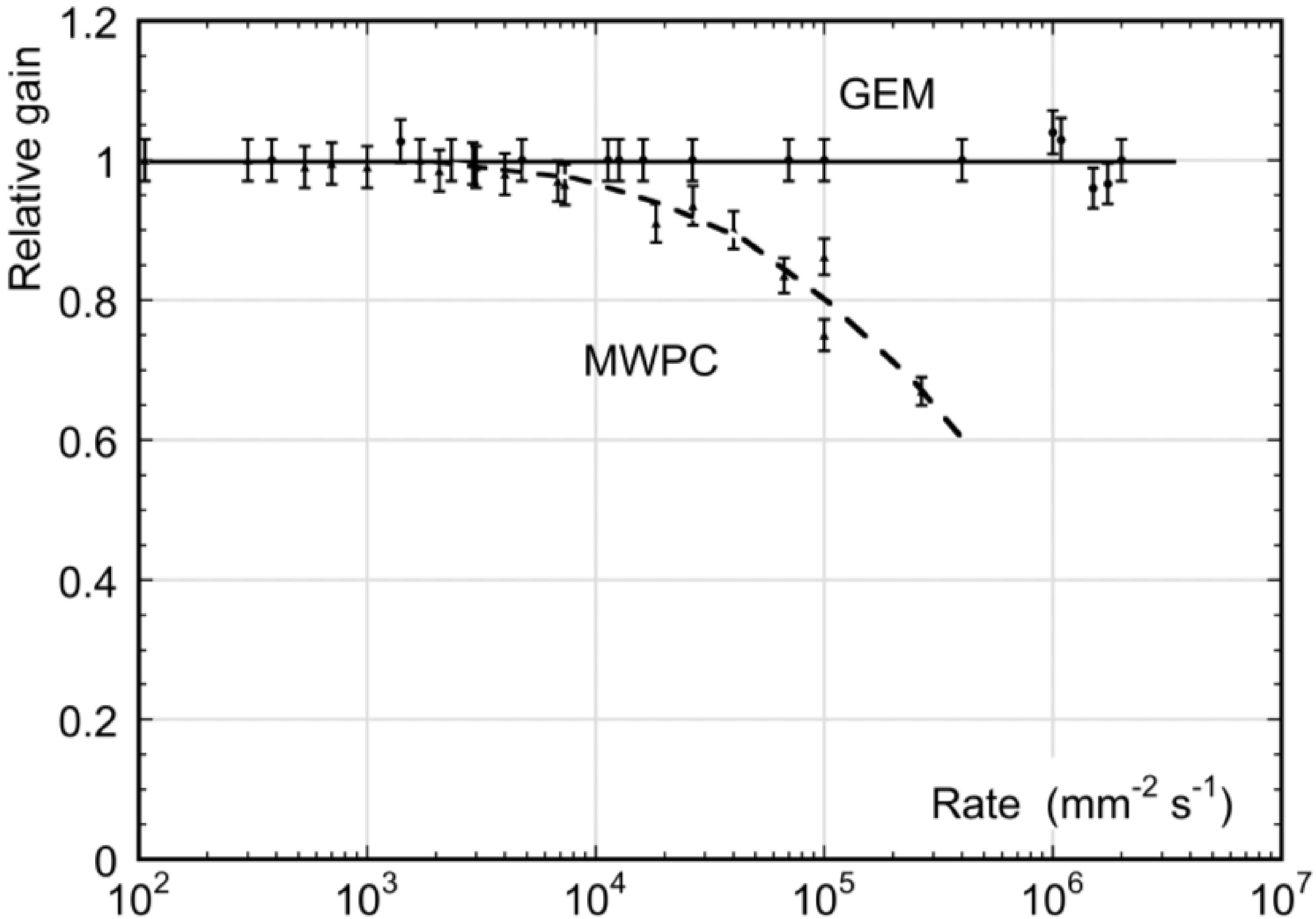

Particle Identification with a Ring Imaging Cherenkov Counter

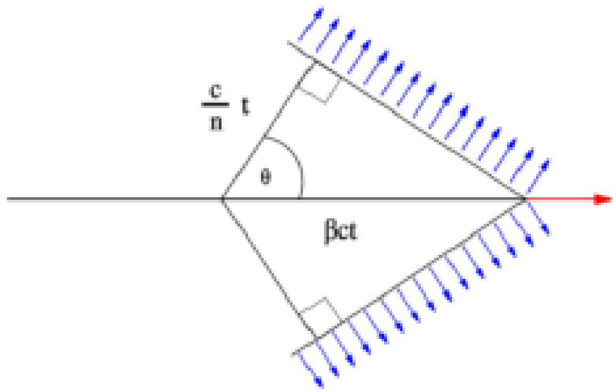

Geometry of Cherenkov radiation: the particle (red arrow) travels in a medium with refractive index n

Charged particles with known momentum can be indetified thanks to the Cherenkov effect:

$$\left.\begin{aligned} \cos\theta_C &= \frac{1}{\beta n} \\ p &= mc\gamma\beta \end{aligned}\right\} \Rightarrow m = p\sqrt{n^2\cos^2\theta_C - 1} \tag{1}$$

Focusing RICH

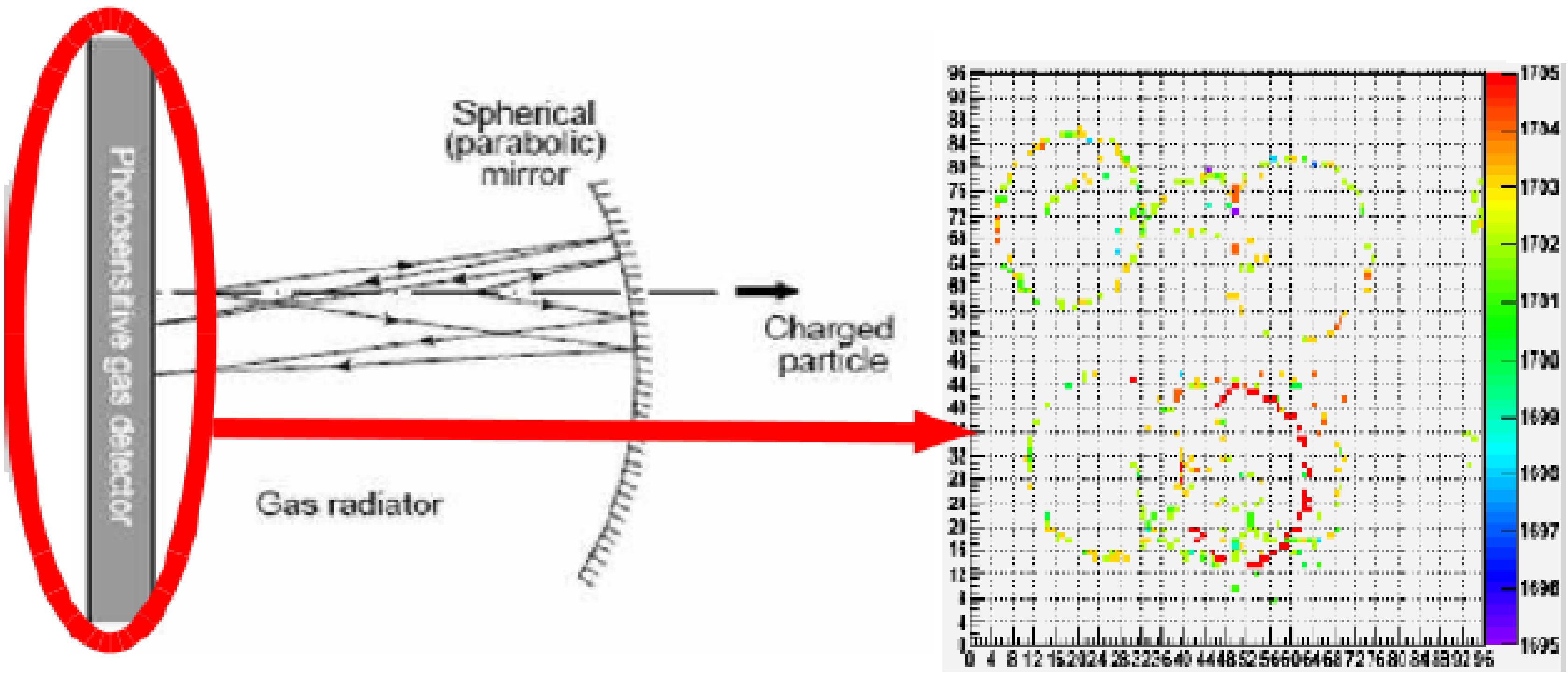

Figure : Focusing scheme: Cherekov photons, collected by a mirror of focal length f, are focused onto the photon detectors placed at the focal plane of the mirror.
The resulting pattern is a circle of radius $r = f \cdot tan\theta_c$.

Ring Imaging Cherenkov

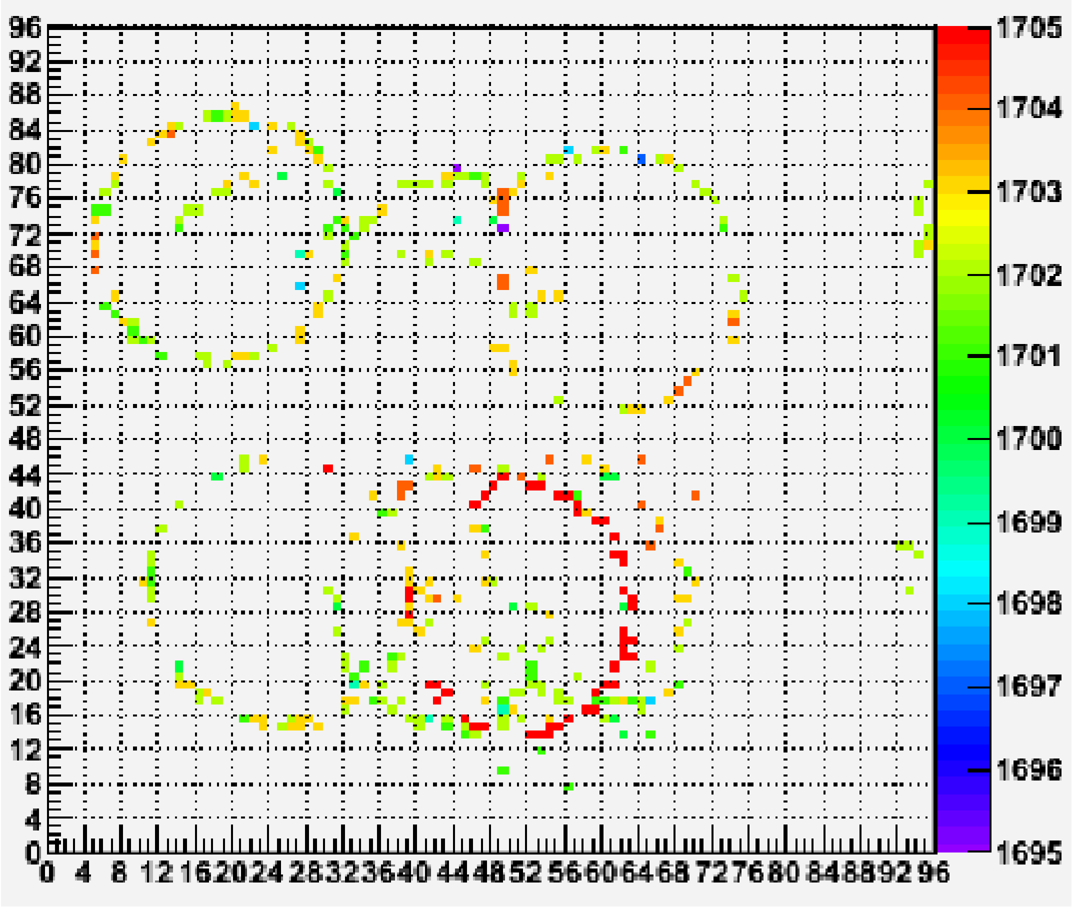

Polya distribution

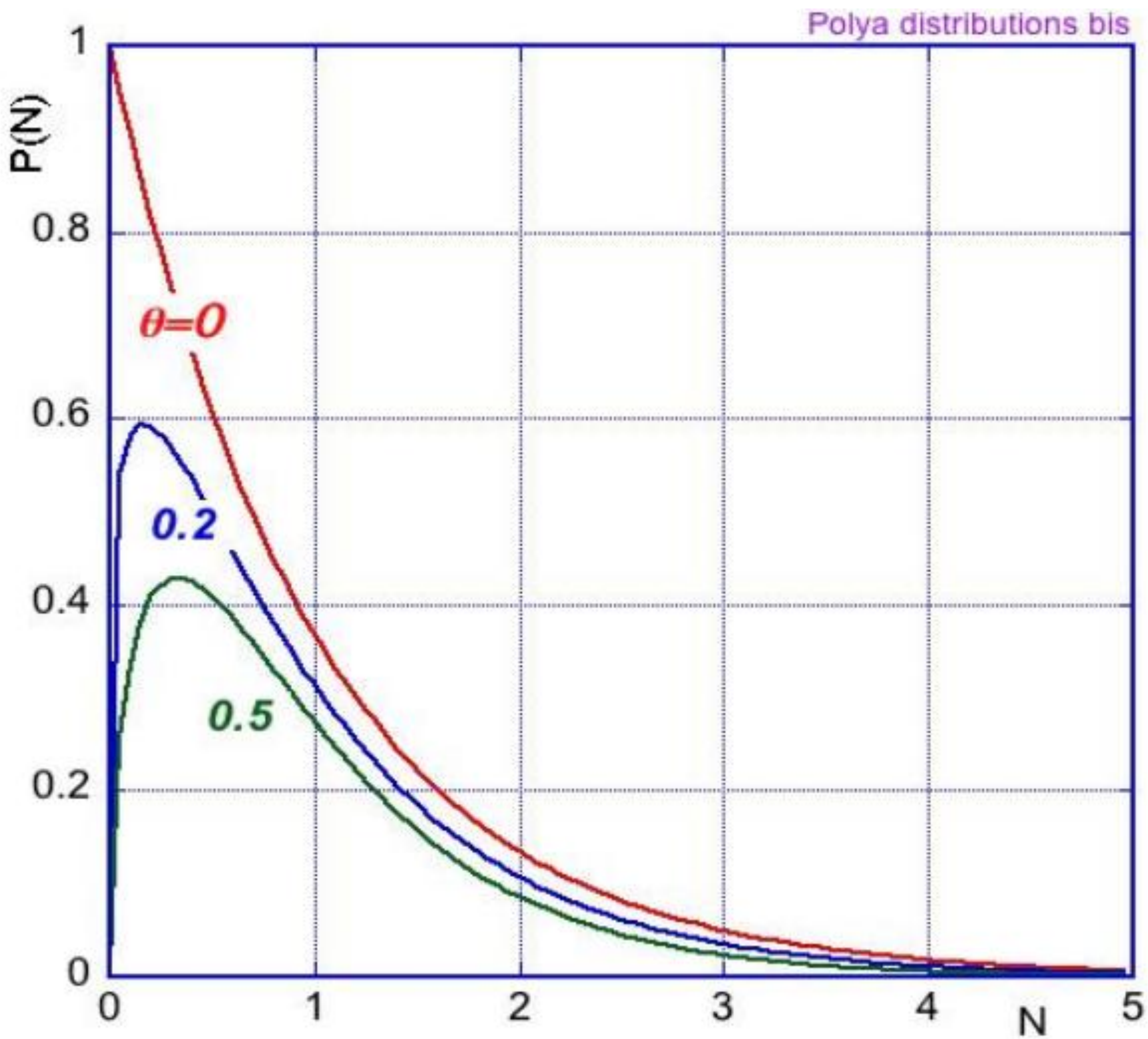

The relevance of high gains for RICH applications

Signal amplitude follows Polya distribution:

$$P(N) = \left(\frac{N(1+\theta)}{\bar{N}}\right)^{\theta} e^{-\frac{N(1+\theta)}{\bar{N}}} \tag{2}$$

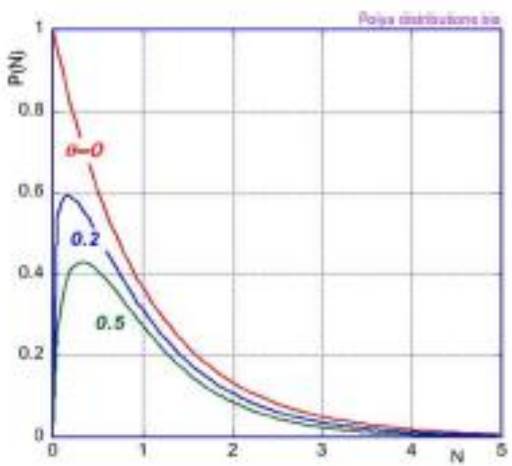

(a)

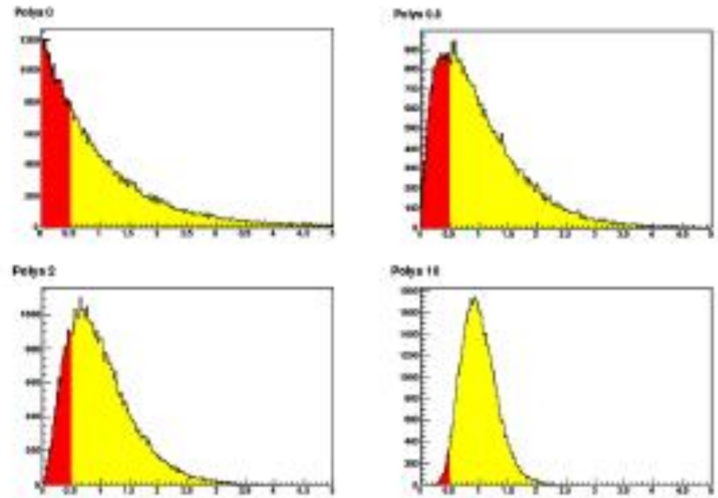

(b)

Figure : Figure (a): Examples of the Polya distributions
Figure (b): Different output spectra for different gain values with a hypothetical threshold of 0.5 (red shadowed areas).
(from PhD Thesis of my Co-Supervisor Stefano Levorato)

Photon Detectors

Photon detectors belong to three families:

- **Vacuum-based (PMTs)**
- **Solid state**
- **Gaseous detectors**

PMTs offer: high rate capability, compactness, robustness and have low noise level. Big drawbacks:

- magnetic field sensitivity
- high cost per channel

Gaseous Photon Detectors are not commercially available
BUT they have specific and unique characteristics:

- **most cost-effective solution to cover very large areas**
- **magnetic insensitive**

MWPCs with CsI photocathodes based PDs

Their performances are limited due to their open geometry:

- **Photon Feedback** $\Rightarrow$ afterpulses and electrical instabilities
- **Ion BackFlow (IBF)** $\Rightarrow$ photocathode aging by ion bombardment

Therefore:

The detectors must be operated at low gain!

Consequencies:

- limitation in single photoelectron detection efficiency
- long integration time of the signal is needed ($\simeq 100ns$)

$\Rightarrow$ Detector memory: these PDs are not adequate for very high rates.

The hybrid MPGD PD scheme

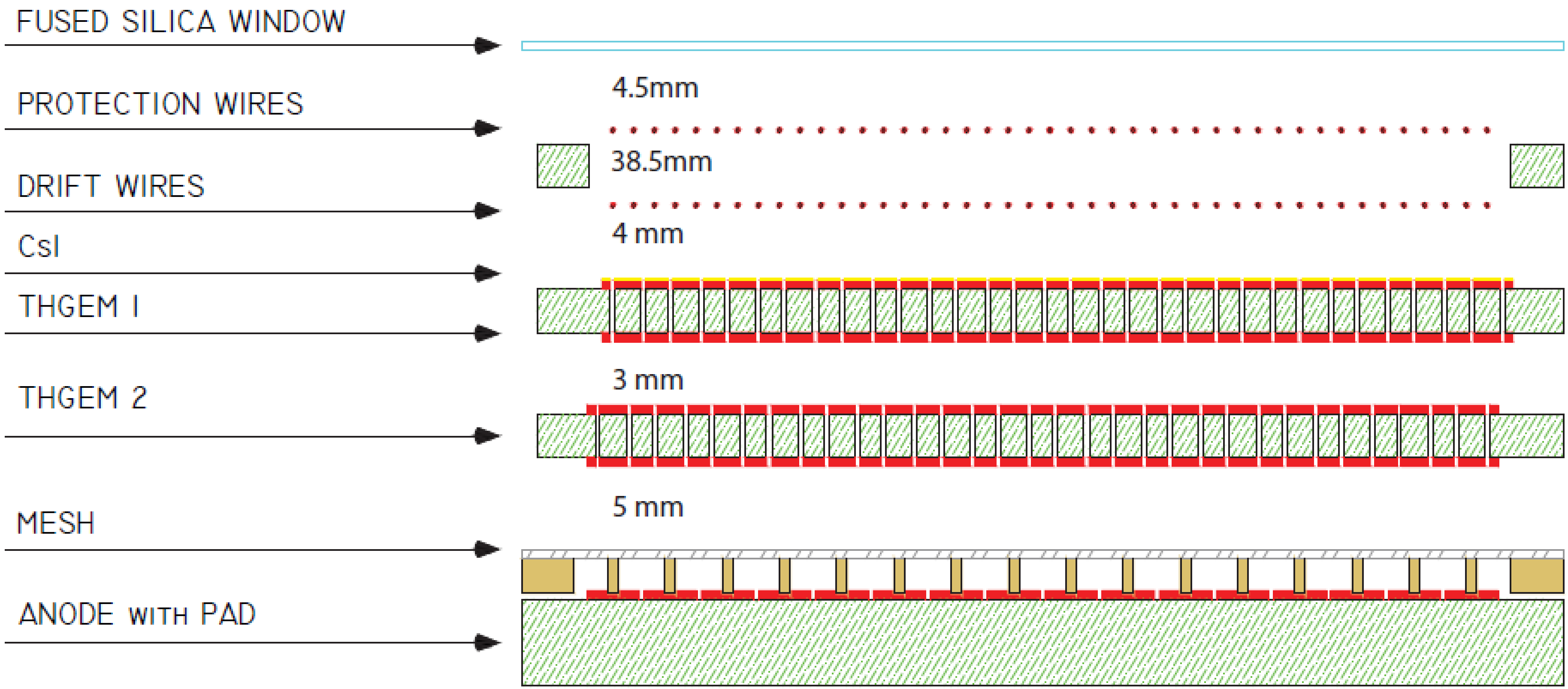

Difficulties faced during the measurements

$Ar:CH_4$ 50:50

Flushing in the morning due to safety protocol

Charge-up effect

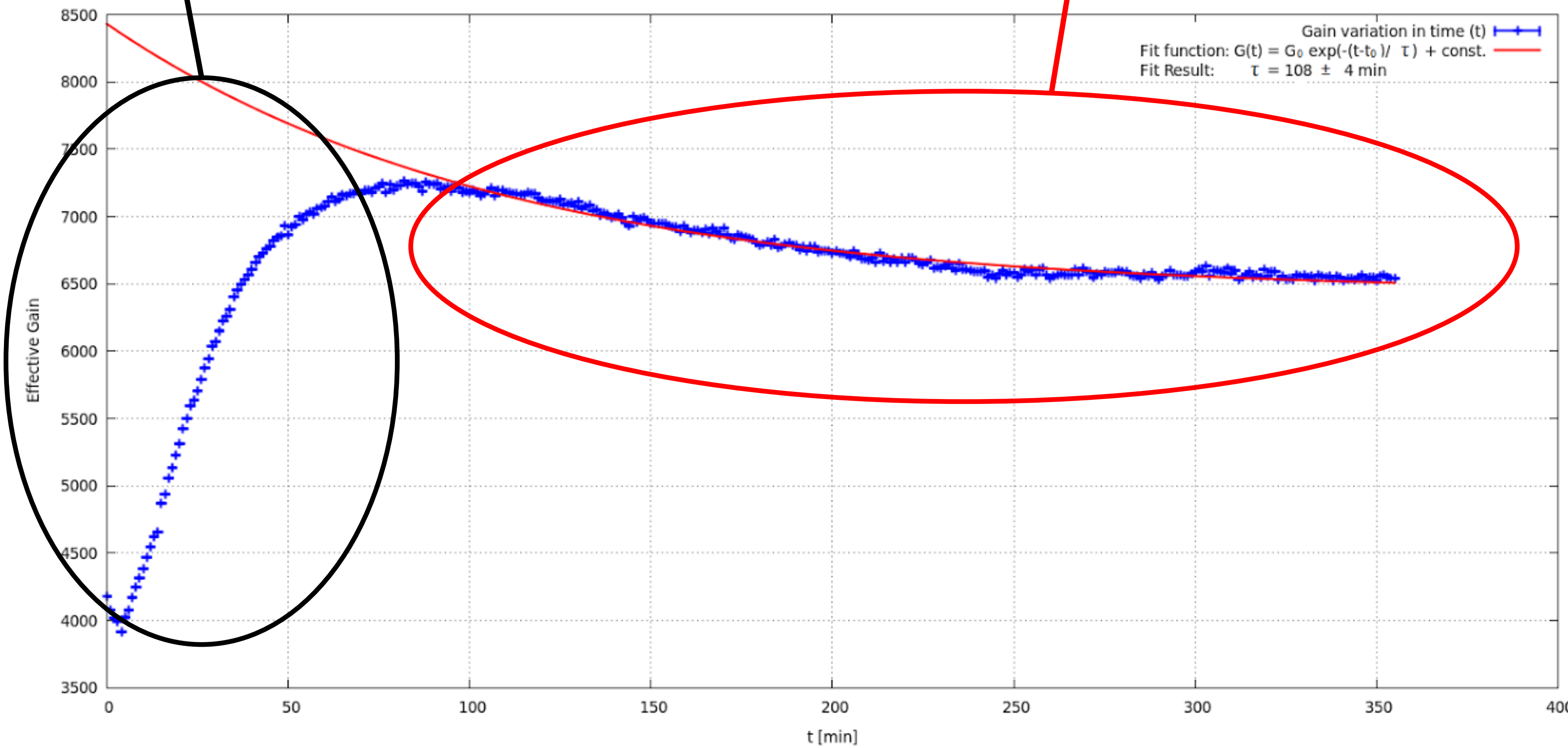

Difficulties faced during the measurements

Charge-up effect

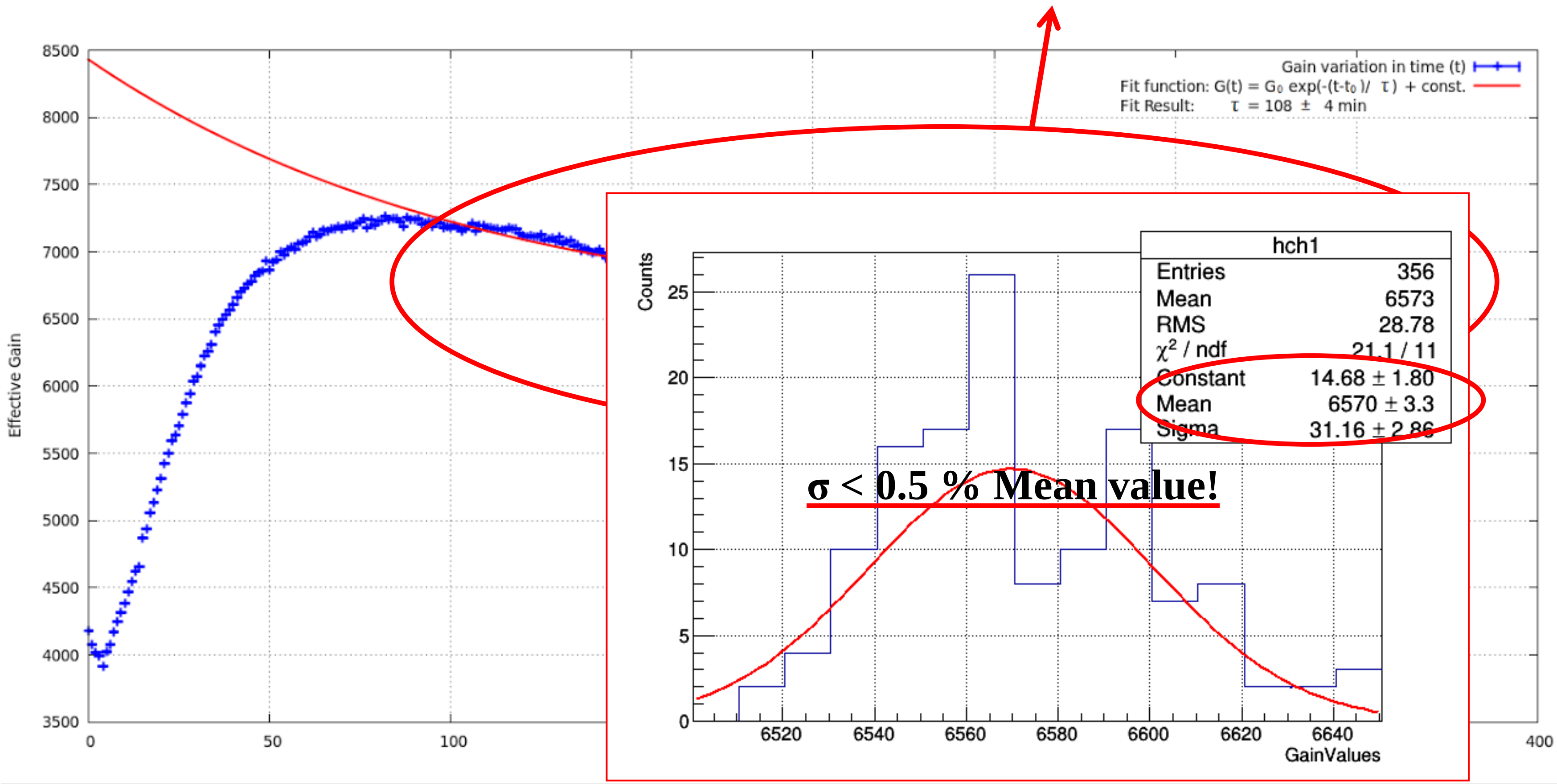

Setup for Pressure measurements

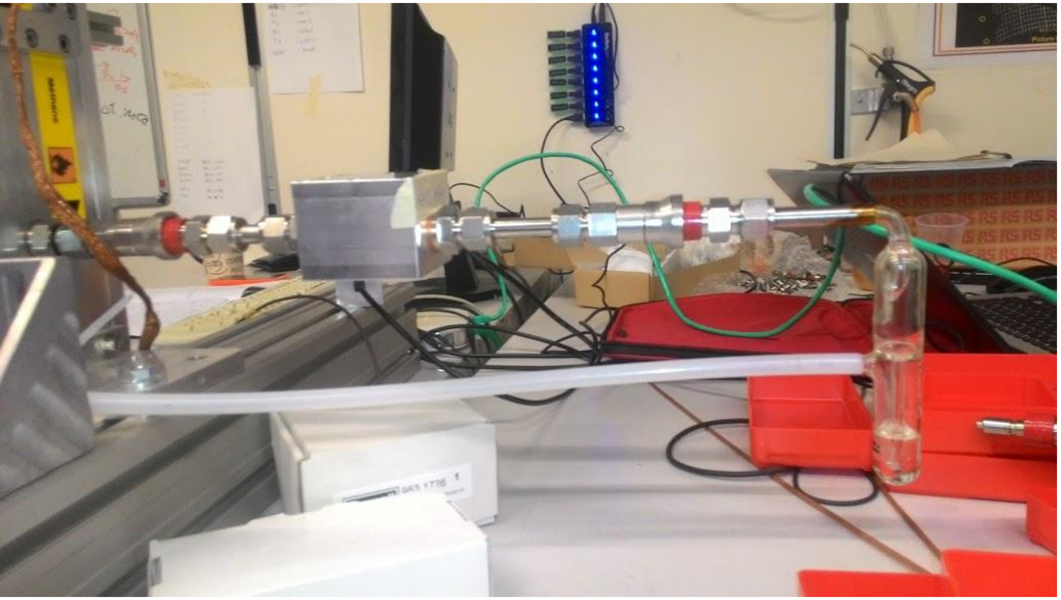

Vplot Graphical User Interface

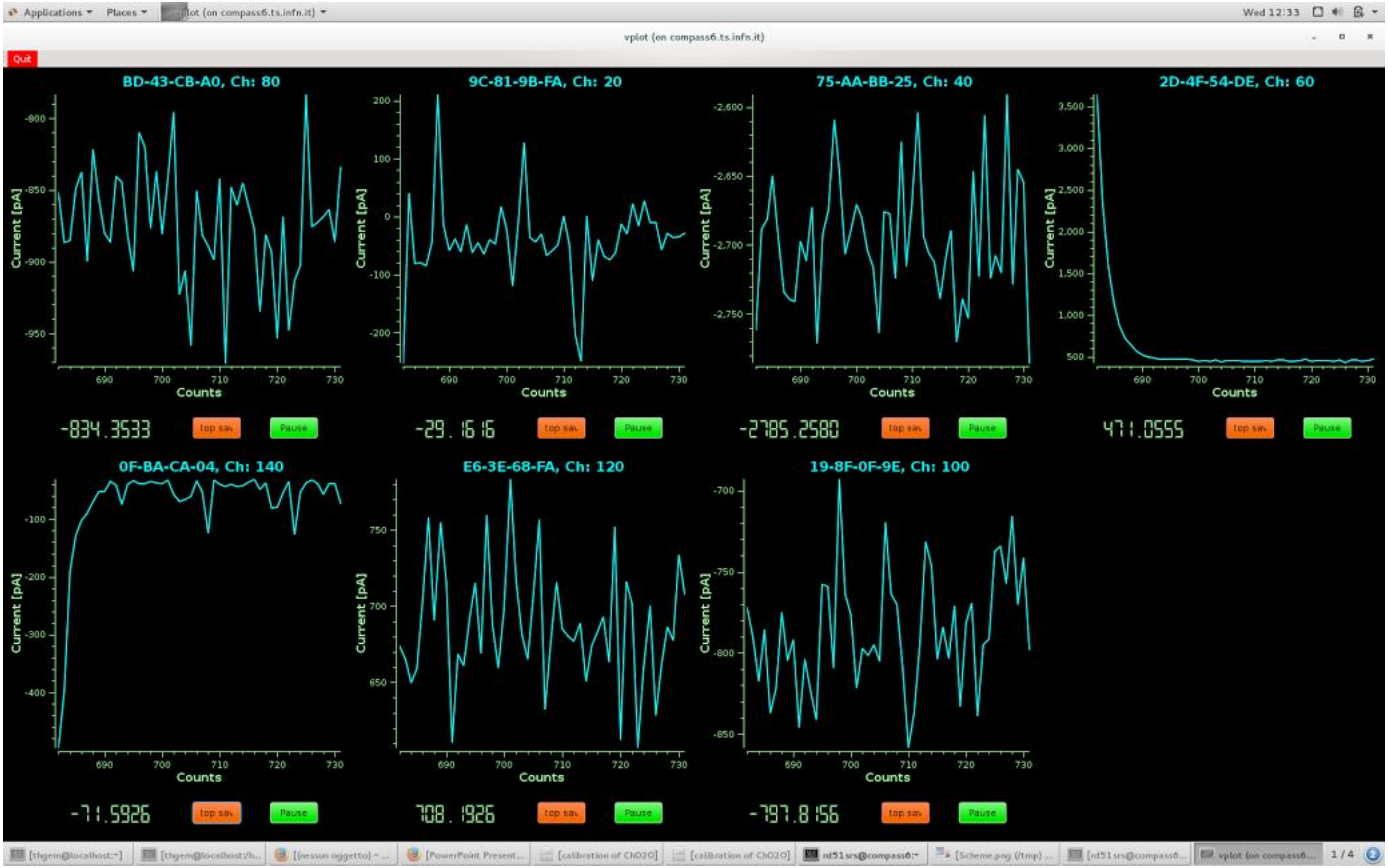

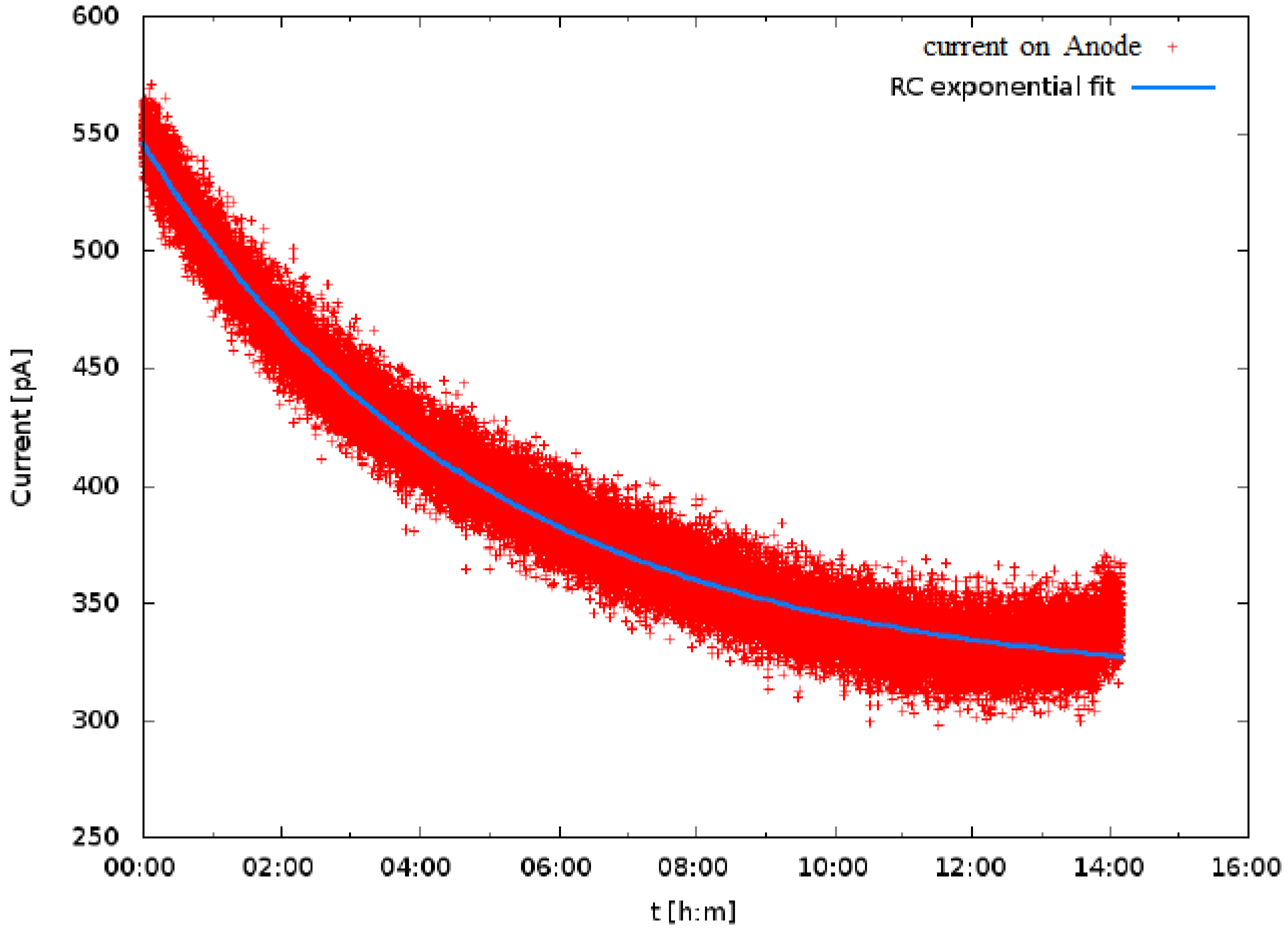
current on Anode
RC exponential fit
Current [pA]
t [h:m]
600
550
500
450
400
350
300
250
00:00
02:00
04:00
06:00
08:00
10:00
12:00
14:00
16:00

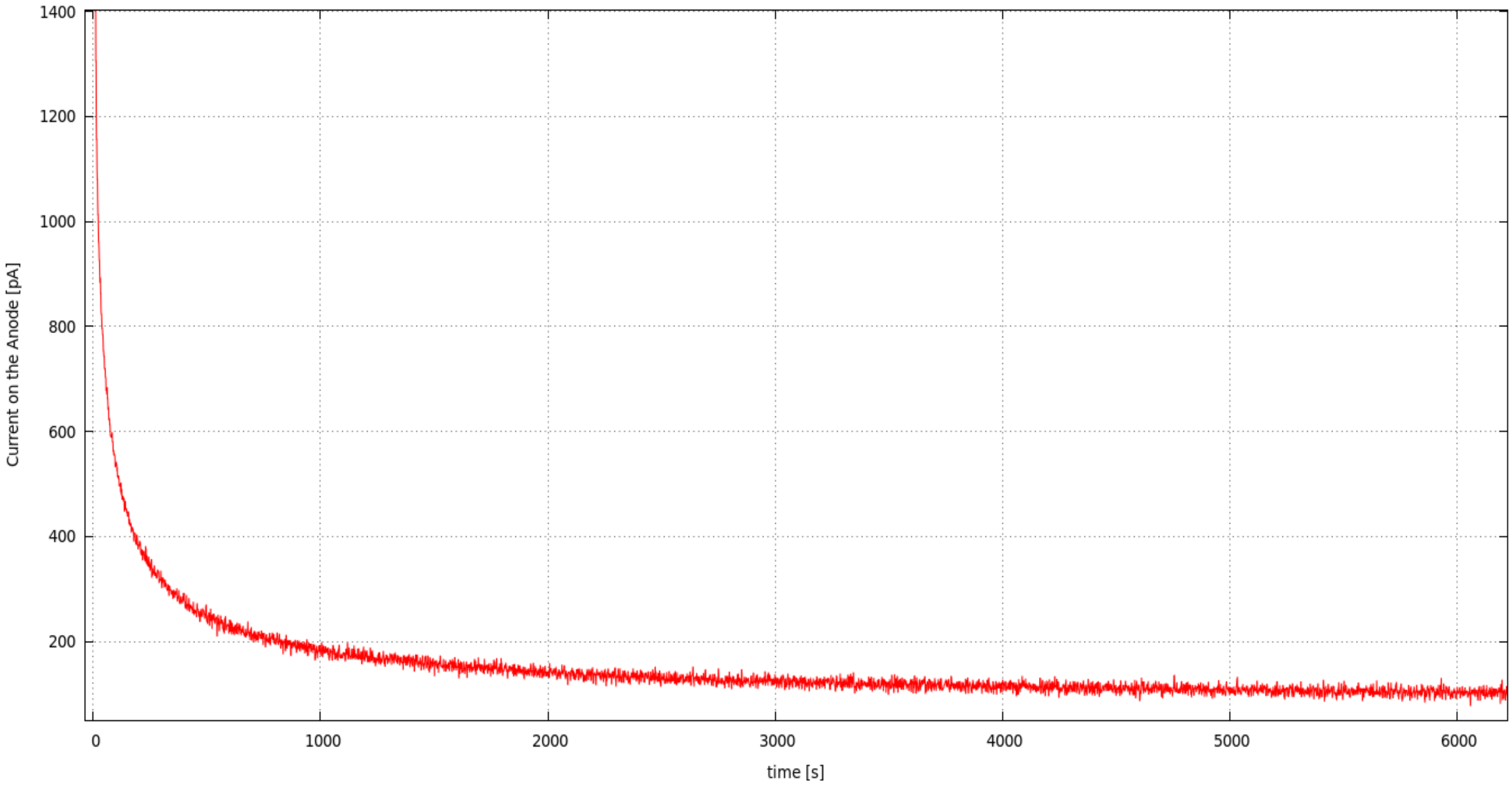
1400
1200
1000
800
600
400
200
Current on the Anode [pA]
0
1000
2000
3000
4000
5000
6000
time [s]

Conclusions

Concerning the measurements of effective gain:

- **Dependence of the gain on the various electric fields has been studied**
- **An universal shape for the collection efficiency of the detector for X-ray ionization has been obtained and a receipe for the maximum collection efficiency has been derived**
- **The rule for keeping a maximum collection efficiency allowed to sucessfully disentangle the individual contributions to the total effective gain**
- **The optimal gain sharing has been studied**
- **The pressure dependence of the gain has been studied, obtaining the factor useful to provide pressure-independent gain values**